

Investigation of PM_{2.5} dispersion in Din Daeng district, Bangkok using Computational
Fluid Dynamics modeling



A Thesis Submitted in Partial Fulfillment of the Requirements
for the Degree of Master of Engineering in Chemical Engineering

Department of Chemical Engineering

FACULTY OF ENGINEERING

Chulalongkorn University

Academic Year 2021

Copyright of Chulalongkorn University

การศึกษาการกระจายของ PM_{2.5} ในเขตดินแดง, กรุงเทพมหานคร โดยใช้แบบจำลองพลศาสตร์ของ
ไหลเชิงคำนวณ



วิทยานิพนธ์นี้เป็นส่วนหนึ่งของการศึกษาตามหลักสูตรปริญญาวิศวกรรมศาสตรมหาบัณฑิต
สาขาวิชาวิศวกรรมเคมี ภาควิชาวิศวกรรมเคมี
คณะวิศวกรรมศาสตร์ จุฬาลงกรณ์มหาวิทยาลัย
ปีการศึกษา 2564
ลิขสิทธิ์ของจุฬาลงกรณ์มหาวิทยาลัย

Thesis Title Investigation of PM_{2.5} dispersion in Din Daeng district,
Bangkok using Computational Fluid Dynamics modeling
By Miss Amintra Tancharoen
Field of Study Chemical Engineering
Thesis Advisor PIMPORN PONPESH

Accepted by the FACULTY OF ENGINEERING, Chulalongkorn University in
Partial Fulfillment of the Requirement for the Master of Engineering

THESIS COMMITTEE

..... Dean of the FACULTY OF
ENGINEERING
(SUPOT TEACHAVORASINSKUN)

..... Chairman
(SUPAREAK PRASERTHDAM)

..... Thesis Advisor
(PIMPORN PONPESH)

..... Examiner
(PHUET PRASERTCHAROENSUK)

..... Examiner
(SOMPONG PUTIVISUTISAK)

..... External Examiner
(Tonkid Chantrasmi)

อminatรา ต้นเจริญ : การศึกษาการกระจายของ $PM_{2.5}$ ในเขตดินแดง, กรุงเทพมหานคร โดยใช้แบบจำลองพลศาสตร์ของไหลเชิงคำนวณ. (Investigation of $PM_{2.5}$ dispersion in Din Daeng district, Bangkok using Computational Fluid Dynamics modeling) อ.ที่ปรึกษาหลัก : พิมพ์พร พลเพชร

ดินแดงเป็นเขตขนาดเล็กและมีประชากรอาศัยอย่างหนาแน่นของกรุงเทพมหานคร ทำให้ความเข้มข้น $PM_{2.5}$ ในเขตดินแดงเกินมาตรฐานรายวันและประจำปีของมาตรฐานคุณภาพอากาศ ในงานวิจัยนี้พลศาสตร์ของไหลเชิงคำนวณ (CFD) ถูกนำมาใช้เพื่อตรวจสอบผลกระทบของลักษณะเมืองและปริมาณการจราจรต่อการกระจายตัวของ $PM_{2.5}$ ในเขตดินแดง โดยใช้แบบจำลอง Standard k- ϵ มีการศึกษาสองสถานการณ์ในงานวิจัยนี้ หนึ่งคือการตรวจสอบอิทธิพลของการมีทางพิเศษและการปล่อย $PM_{2.5}$ ที่เกิดขึ้น อีกประการหนึ่งคือการตรวจสอบอิทธิพลของการระบาดของโรค COVID-19 ที่ส่งผลกระทบต่อปริมาณการจราจร จากผลการจำลองแสดงให้เห็นถึงการมีอยู่ของทางพิเศษในเขตดินแดงเพิ่มความเข้มข้นของ $PM_{2.5}$ เมื่อมีทางพิเศษจะเพิ่มความเข้มข้นของ $PM_{2.5}$ ขึ้นประมาณ 3.4 เท่า เมื่อเทียบกับกรณีไม่มีทางพิเศษ การระบาดของโรค COVID-19 จะส่งผลกระทบต่อความเข้มข้นของ $PM_{2.5}$ ในระหว่างการล็อคดาวน์นั้น ความเข้มข้นของ $PM_{2.5}$ ลดลงประมาณ 63% เมื่อเทียบกับช่วงเวลาปกติ



สาขาวิชา วิศวกรรมเคมี
ปีการศึกษา 2564

ลายมือชื่อนิสิต
ลายมือชื่อ อ.ที่ปรึกษาหลัก

6370326621 : MAJOR CHEMICAL ENGINEERING

KEYWORD: PM_{2.5} Dispersion, Computational Fluids Dynamics, Traffic, Street
Canyon, Bangkok

Amintra Tancharoen : Investigation of PM_{2.5} dispersion in Din Daeng district,
Bangkok using Computational Fluid Dynamics modeling. Advisor: PIMPORN
PONPESH

Din Daeng is a small and densely populated district of Bangkok with two major expressways in the area. PM_{2.5} concentrations in Din Daeng district often exceed both daily and annual standards of the National Ambient Air Quality Standards. Computational Fluid Dynamics (CFD) was applied to investigate the effects of the metropolitan characteristics and traffic volumes on the dispersion of PM_{2.5} in Din Daeng district. The turbulent flow was analyzed using the Standard k- ϵ model. There are two scenarios in this simulation study. One is to investigate the consequences of having the expressways and their resulting PM_{2.5} emissions. The other is to examine the influence of the COVID-19 pandemic and the city lockdown which affected the traffic volumes. The presence of the expressways in Din Daeng district was demonstrated to enhance PM_{2.5} concentrations. The presence of the expressway increased the concentration of PM_{2.5} by approximately 3.4 times compared to the case of no expressways. The COVID-19 pandemic seemed to have an impact on the concentration of PM_{2.5} during the city lockdown. During the city lockdown, the concentration of PM_{2.5} was reduced by approximately 63% compared to the normal period.

Field of Study: Chemical Engineering

Student's Signature

Academic Year: 2021

Advisor's Signature

ACKNOWLEDGEMENTS

This thesis becomes successful with the support of the thesis advisor, Assistant Professor Dr. Pimporn Ponpesh, who kindly provided suggestions and opinions that would be helpful in the implementation as well as improving and rectifying problems.

I would like to thank the Traffic and Transportation Department, Air Quality and Noise Management Division of Bangkok, Expressway Authority of Thailand, Pollution Control Department, Department of City planning and Urban Development, and Dr.Ornicha Anuchitchanchai from the transportation institute at Chulalongkorn university for kindly providing the data essential for this thesis.

Finally, thank you to my family, seniors, and friends for all their help and support throughout this thesis. I would not have achieved this far and this thesis would not have been completed without all the support that I have always received from them.

Amintra Tancharoen



จุฬาลงกรณ์มหาวิทยาลัย
CHULALONGKORN UNIVERSITY

TABLE OF CONTENTS

	Page
ABSTRACT (THAI).....	iii
ABSTRACT (ENGLISH).....	iv
ACKNOWLEDGEMENTS.....	v
TABLE OF CONTENTS.....	vi
LIST OF TABLES.....	ix
LIST OF FIGURES.....	xv
Chapter 1 Introduction.....	1
1.1 Introduction.....	1
1.2 Objectives.....	2
1.3 The scope of research.....	3
Chapter 2 Theories and Literature reviews.....	4
2.1 Urban Street Canyon.....	4
2.1.1 Geometry and classification.....	4
2.2 Navier-Stokes Equations.....	5
2.2.1 Equation.....	6
2.2.1.1 Conservation of mass.....	6
2.2.1.2 Conservation of momentum.....	6
2.2.1.3 Conservation of energy.....	8
2.3 Standard k-epsilon turbulence model.....	8
2.4 Discrete Phase Model.....	9
2.5 Literature Reviews.....	11

Chapter 3 Methodology	15
3.1 Preparing the necessary information.....	17
3.2 Study area.....	18
3.3 Model Simulation.....	19
3.3.1 Geometric Model.....	19
3.3.2 Computational domain	20
3.3.3 Generic mesh.....	21
3.3.4 Setup.....	27
Chapter 4 Results and Discussion	49
4.1 Model Validation	49
4.1.1 Discrete Phase Model Validation Results: January 27 2020 (Normal period).....	49
4.1.2 Discrete Phase Model Validation Results: January 25 2021 (Lockdown period).....	50
4.2 The influence of the expressways.....	60
4.3 The influence of the city lockdown due to COVID-19 pandemic.....	79
Chapter 5 Conclusion	83
5.1 Validation Modal	83
5.2 Studies on the dispersion of PM _{2.5} when there are expressways.....	84
5.3 Studies on the dispersion of PM _{2.5} during normal and lockdown periods.	84
5.4 Propose a guideline solution.....	84
5.5 Limitations	85
REFERENCES	86
VITA.....	91



จุฬาลงกรณ์มหาวิทยาลัย
CHULALONGKORN UNIVERSITY

LIST OF TABLES

	Page
Table 1: PM _{2.5} values in the area along Din Daeng Road, Din Daeng District, 2019.....	15
Table 2: PM _{2.5} values in the area along Din Daeng Road, Din Daeng District, 2020.....	16
Table 3: PM _{2.5} values in the area along Din Daeng Road, Din Daeng District, 2021.....	16
Table 4: Data for simulations and sources.	18
Table 5: Details of mesh.....	21
Table 6: Detail of mesh on four edges of the domain.	23
Table 7: Detail of mesh in the three roads.	23
Table 8: Detail of mesh in the residence building area.....	24
Table 9: Detail of mesh around both expressway lines.	24
Table 10: The quality and amount of mesh in the case of the expressways.....	25
Table 11: The quality and amount of mesh in the case of no expressways.	26
Table 12: Constants used in the Standard k - ϵ Model.....	29
Table 13: Emission factor for each vehicle type. (EMEP/EEA, 2006).....	30
Table 14: The lengths of roads and expressways in the model.	30
Table 15: Traffic volume from 7 AM – 9 AM around Din Daeng Road and Traffic volume from 6:30 AM - 9 AM on Pracha Songkhro and Mitmaitri Roads during normal period.....	31
Table 16: Traffic volume from 9 AM – 4 PM around Din Daeng, Pracha Songkhro, and Mitmaitri Roads during the normal period.	32
Table 17: Traffic Volume of the Chalerm Mahanakhon and the Si Rat Expressways during the normal period.....	34

Table 18: Traffic volume from 7 AM – 9 AM around Din Daeng Road and traffic volume from 6.30 AM – 9 AM in Pracha Songkhro, and Mitmaitri Roads during the lockdown period.....	35
Table 19: Traffic volume from 9 AM. – 4 PM on Din Daeng, Pracha Songkhro, and Mitmaitri Roads during the lockdown period.	37
Table 20: Traffic Volume of the Chalerm Mahanakorn and the Si Rat Expressways during the lockdown period.....	39
Table 21: A summary of the emission rates used in simulations during the normal period.....	40
Table 22: A summary of emission rates used in the simulations during the lockdown period.....	41
Table 23: Wind direction is used in both normal and lockdown periods.....	42
Table 24: Mean wind speed is used in both normal and lockdown periods.....	43
Table 25: Turbulence Setup.....	43
Table 26: Hydraulic Diameter in both cases with/without expressways.	44
Table 27: Mean temperatures are used in simulations for both normal and lockdown periods.	45
Table 28: Outlet Momentum Settings.....	46
Table 29: Roads, Expressways, and Ground Momentum Settings.	47
Table 30: Mean Road temperatures are used in both normal and lockdown periods.	47
Table 31: Method Settings.	48
Table 32: Control Settings.....	48
Table 33: A comparison of PM _{2.5} concentrations on January 27, 2020, from 7 AM - 9 AM.....	49
Table 34: A comparison of temperatures on January 27, 2020, from 7 AM - 9 AM....	49

Table 35: A comparison of wind speeds on January 27, 2020, from 7 AM - 9 AM.	49
Table 36: A comparison of PM _{2.5} concentrations on January 27, 2020, from 10 AM - 12 PM.	50
Table 37: A comparison of temperatures on January 27, 2020, from 10 AM - 12 PM.	50
Table 38: A comparison of wind speeds on January 27, 2020, from 10 AM - 12 PM.	50
Table 39: A comparison of PM _{2.5} concentrations on January 25, 2021, from 7 AM – 9 AM.	51
Table 40: A comparison of temperatures on January 25, 2021, from 7 AM – 9 AM... ..	51
Table 41: A comparison of wind speeds on January 25, 2021, from 7 AM – 9 AM. ...	51
Table 42: A comparison of PM _{2.5} concentrations on January 25, 2021, from 10 AM – 12 PM.	51
Table 43: A comparison of temperatures on January 25, 2021, from 10 AM – 12 PM.	52
Table 44: A comparison of wind speeds on January 25, 2021, from 9 AM – 12 PM. .	52
Table 45: A comparison of PM _{2.5} concentrations on January 25, 2021, from 1 PM – 4 PM.	52
Table 46: A comparison of temperatures on January 25, 2021, from 1 PM – 4 PM... ..	52
Table 47: A comparison of wind speeds on January 25, 2021, from 1 PM – 4 PM.....	53
Table 48: PM _{2.5} concentrations at the air quality monitoring station were compared to the results obtained from the three time periods on January 27, 2020.....	53
Table 49: PM _{2.5} concentrations at the air quality monitoring station were compared to the results obtained from the three time periods on January 25, 2021.....	53
Table 50: Multiply the correction factor by 0.00326 so that the simulation results are close to the values obtained at the air quality monitoring station on January 27, 2020.....	55

Table 51: Temperatures at the air quality monitoring station were compared with the simulation results obtained from the three time periods on January 27, 2020....	56
Table 52: Velocities at the air quality monitoring station were compared with the simulation results obtained from the three time periods on January 27, 2020.	56
Table 53: Multiply the correction factor by 0.00326 so that the simulation results are close to the values obtained at the air quality monitoring station on January 25, 2021	57
Table 54: Temperatures at the air quality monitoring station were compared with the simulation results obtained from the three time periods on January 25, 2021....	58
Table 55: Velocities at the air quality monitoring station were compared with the simulation results obtained from the three time periods on January 25, 2021.	59
Table 56: A comparison of PM _{2.5} concentrations on January 27, 2020, from 7 AM – 9 AM when there are no expressways.....	61
Table 57: A comparison of temperatures on January 27, 2020, from 7 AM – 9 AM when there are no expressways.....	61
Table 58: A comparison of wind speeds on January 27, 2020, from 7 AM – 9 AM when there are no expressways.....	61
Table 59: A comparison of PM _{2.5} concentrations on January 27, 2020, from 10 AM – 12 PM when there are no expressways.....	62
Table 60: A comparison of temperatures on January 27, 2020, from 10 AM – 12 PM when there are no expressways.....	62
Table 61: A comparison of wind speeds on January 27, 2020, from 10 AM – 12 PM when there are no expressways.....	62
Table 62: PM _{2.5} concentrations at the air quality monitoring station were compared to the results without expressways obtained from three time periods on January 27, 2020.....	63

Table 63: Multiply the correction factor by 0.00326 so that the simulation results without expressways are close to the values obtained at the air quality monitoring station on January 27, 2020.	63
Table 64: Temperatures at the air quality monitoring station were compared with the simulation results without expressways obtained from the three time periods on January 27, 2020.	64
Table 65: Velocities at the air quality monitoring station were compared with the simulation results without expressways obtained from the three time periods on January 27, 2020.	65
Table 66: PM _{2.5} concentrations at the air quality monitoring station compared to the simulation results obtained from the three time periods. The results obtained from simulation multiply correction factor equal to 0.00326 to make the value close to the measured value from the air quality monitoring station.	66
Table 67: Temperatures at the air quality monitoring station were compared to the simulation results obtained from the three time periods.	68
Table 68: Velocities at the air quality monitoring station were compared to the simulation results obtained from the three time periods.	69
Table 69: Wind speed, wind direction, and emission rate in each period.	71
Table 70: Emission rate and simulated meteorological results for the area near the expressway on Jan 27, 2020.	74
Table 71: A comparative result of PM _{2.5} concentrations of both simulations at the measurement point of the high-rise building.	77
Table 72: Comparative results of PM _{2.5} concentrations of both simulations at locations where PM _{2.5} concentrations were measured at different distances from the road.	79
Table 73: Comparative results of PM _{2.5} concentration during normal and lockdown periods.	80

Table 74: Wind speed and wind direction for three periods of normal and lockdown periods. 81

Table 75: Wind speed and wind direction for three periods of normal and lockdown periods. 81

Table 76: Emission rate, normal and lockdown periods..... 82



LIST OF FIGURES

	Page
Figure 1: Urban Street Canyon (T.R., 1998).	4
Figure 2: Focused area for the investigation of PM _{2.5} dispersion in Din Daeng.	19
Figure 3: Geometry of the focused area.....	20
Figure 4: Structure of expressway.....	20
Figure 5: Computational domain of the focused area.	21
Figure 6: Mesh of CFD simulation (front view).	25
Figure 7: Mesh of CFD simulation (side view).....	25
Figure 8: Setting Fluent Launcher (Setting Edit Only).....	28
Figure 9: Setting Solver.....	28
Figure 10: Gravitational Acceleration.....	28
Figure 11: Setting injections.....	29
Figure 12: Setting inlet boundary conditions.....	41
Figure 13: Wind direction from 7 AM – 4 PM.....	42
Figure 14: The width and height of the study area in the presence of expressways. 43	
Figure 15: The width and height of the study area in the absence of expressways... 44	
Figure 16: Inlet Temperature Setting.....	45
Figure 17: Inlet DPM Settings.	46
Figure 18: Relationship between PM _{2.5} concentrations from measurement data and simulation results.	54
Figure 19: A comparison between the PM _{2.5} concentrations measured at the air quality monitoring station and the simulation results on January 27, 2020.	55

Figure 20: A comparison between the temperatures measured at the air quality monitoring station and the simulation results on January 27, 2020.	56
Figure 21: A comparison between the velocities measured at the air quality monitoring station and the simulation results on January 27, 2020.	57
Figure 22: A comparison between the PM _{2.5} concentrations measured at the air quality monitoring station and the simulation results on January 25, 2021.	58
Figure 23: A comparison between the temperatures measured at the air quality monitoring station and the simulation results on January 25, 2021.	59
Figure 24: A comparison between the velocities measured at the air quality monitoring station and the simulation results on January 25, 2021.	60
Figure 25: A comparison between the PM _{2.5} concentrations measured at the air quality monitoring station and the simulation results without expressways on January 27, 2020.	64
Figure 26: A comparison between the temperatures measured at the air quality monitoring station and the simulation results without expressways on January 27, 2020.	65
Figure 27: A comparison between the velocities measured at the air quality monitoring station and the simulation results without expressways on January 27, 2020.	66
Figure 28: A comparison between PM _{2.5} concentrations measured at the air quality monitoring station and the values obtained from the simulation results in both cases.	67
Figure 29: A comparison between temperatures measured at the air quality monitoring station and the values obtained from the simulation results in both cases.	68
Figure 30: A comparison between velocities measured at the air quality monitoring station and the values obtained from the simulation results in both cases.	69

Figure 31: PM _{2.5} concentrations in the whole numerical model at 7 AM – 9 AM in the case of expressways.....	70
Figure 32: PM _{2.5} concentrations in the whole numerical model at 10 AM – 12 PM in the case of expressways.	70
Figure 33: PM _{2.5} concentrations in the whole numerical model at 7 AM – 9 AM in the case of no expressways.....	72
Figure 34: PM _{2.5} concentrations in the whole numerical model at 10 AM – 12 PM in the case of no expressways.	72
Figure 35: Mass flow of PM _{2.5} in Din Daeng district (simulated from traffic volume and meteorological data as of 27 January 2020 at 1-4 PM): (a) with expressways, (b) without expressways.	73
Figure 36: A cross-sectional plane of Mass flow of PM _{2.5} in area A (simulated from traffic volume and meteorological data as of 27 January 2020 at 1-4 PM): (a) with expressways, (b) without expressways.....	73
Figure 37: Airflow fields at the area near the expressway on Din Daeng Road during (a) 7-9 AM, (b) 10 AM – 12 PM, (c) 1-4 PM.....	74
Figure 38: PM _{2.5} concentration contour at the area near the expressway on Din Daeng Road during (a) 7-9 AM, (b) 10 AM – 12 PM, (c) 1-4 PM.	75
Figure 39: Location of PM _{2.5} concentration measurement points at high-rise buildings.	76
Figure 40: A comparison of PM _{2.5} concentrations in both simulations at the measurement point of the high-rise building.....	76
Figure 41: PM _{2.5} dispersion on a cross-sectional plane at the high building during: (a) 10 AM – 12 PM, (b) 1 PM - 4 PM.....	77
Figure 42: Location of concentration measurement points at different distances from the road.....	78

Figure 43: A Comparison of $PM_{2.5}$ concentrations of both simulations at the locations where the $PM_{2.5}$ concentrations were measured at different distances from the road. 78

Figure 44 : $PM_{2.5}$ concentration during normal and lockdown periods near the air quality monitoring station..... 80



Chapter 1

Introduction

1.1 Introduction

Air pollution is currently a big issue in Thailand, especially in Bangkok. Bangkok has seen a severe dust cover phenomenon in recent years. Also known as $PM_{2.5}$, or dust particles as small as 2.5 microns, which is approximately one-quarter of the diameter of a human hair (Ville Miettinen, 2019). Thailand has ruled that the average 24-hour $PM_{2.5}$ concentration should not exceed 50 micrograms per cubic meter (Department, 2020). When $PM_{2.5}$ enters the human body, it affects the function of numerous organs, whether it is a rash. Skin inflammatory diseases Furthermore, long-term exposure to $PM_{2.5}$ raises the risk of coronary heart disease and lung illness. In addition to lung cancer.

Air pollutants from industrial facilities, open-air burning (such as garbage burning, grass burning, etc.), and vehicles are the sources of $PM_{2.5}$ in Bangkok. Vehicles are the primary source of pollution, with 72.5% of $PM_{2.5}$ in Bangkok is emitted from vehicles (Luz T Padró-Martínez et al., 2012). Trucks had the highest percentage at 28%, followed by pickup trucks (21%), personal vehicles (10%), buses (7%), motorcycles (5%), and vans (1.5%) (Sukko, 2020). According to statistics on registered vehicles in Bangkok, every year, there is an increasing tendency. In 2021, the number of vehicle registrations increased by 2.46 percent over the previous year (Transport Statistics Sub-Division, 2021).

Another factor leading to high $PM_{2.5}$ concentrations in Bangkok might be due to Bangkok's characteristics. The structure appears to be a tall structure, such as a hotel or a commercial mall, combined with residences. The streets within the alley are quite narrow. When compared to open regions, some places have electric train structures, resulting in inadequate ventilation.

Din Daeng is one of Bangkok's fifty districts. It has a total area of 8.354 square kilometers as well as a population of 112,814 ((BORA), 2020). Most of the area is

composed of residential buildings, government offices, secondary, vocational, and tertiary educational institutions, as well as commercial areas. Din Daeng's overall area is composed of buildings that are not particularly tall. Din Daeng transportation consists of the Din Daeng Intersection, which has a daily traffic volume of around 30,000 - 33,000 vehicles, and the Pracha Songkhro Intersection. The traffic volume is around 4,000 - 5,000 vehicles per day, whereas the traffic volume at Mitmaitri Intersection is between 8,000 - 11,000 vehicles per day (T. a. T. Department, 2019-2021). The area is served by two expressways, the Chalm Maha Nakhon Expressway, and the Si Rat Expressway. The Chalm Maha Nakhon Expressway has a daily traffic volume of about 300,000 vehicles, and the Si Rat Expressway has a daily traffic volume of about 580,000 vehicles (Administration, 2019-2021).

The investigation of $PM_{2.5}$ dispersion may be accomplished using a variety of methods, including field measurement, wind tunnel, and computational fluid dynamics (CFD). Thus, computational fluid dynamics (CFD) was used in this study. It is the use of algorithms to analyze processes such as flow, heat transport, and particle diffusion. It saves time and money by simulating various conditions that are difficult or impossible in experiments.

1.2 Objectives

- 1.2.1 Develop a model that may be used to simulate the dispersion of $PM_{2.5}$.
- 1.2.2 Using the CFD model, investigate the dispersion of $PM_{2.5}$ and the influence of traffic conditions and other factors.
- 1.2.3 Propose a guideline solution to reduce PM_5 based on the simulation results.

1.3 The scope of research

- 1.3.1 In Din Daeng, collect data such as geographical data, meteorological data, and $PM_{2.5}$ data.
- 1.3.2 Selecting an appropriate model, a simulation may be used to investigate the dispersion of $PM_{2.5}$.
- 1.3.3 Validate the model's accuracy by comparing model results to measurement data.
- 1.3.4 Investigate the dispersion of $PM_{2.5}$ and the effects of various variables.
- 1.3.5 Propose a guideline solution to reduce $PM_{2.5}$



Chapter 2

Theories and Literature reviews

2.1 Urban Street Canyon

Urban Street Canyon is an area where roadways are lined by buildings, making it resemble a valley. As air flows in, it collides with the building and flows into the canyon, generating an air vortex. As seen in Figure 1, the circulation of air inside the canyon conveys dust created by vehicles collecting in the canyon.

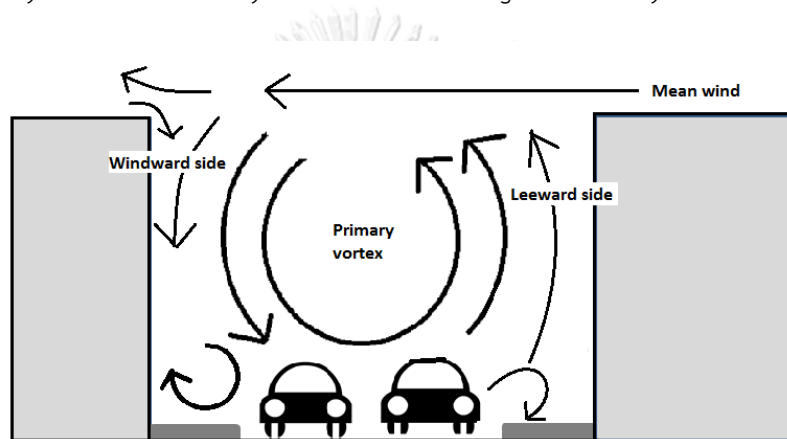


Figure 1: Urban Street Canyon (T.R., 1998).

2.1.1 Geometry and classification

The important geometric ratio is the ratio of the building's height (H) to the width of the road (W), also known as the aspect ratio, which is classified into three categories.

2.1.1.1 Regular canyon has an aspect ratio of approximately 1.

2.1.1.3 Deep canyon: The aspect ratio is approximately 2.

There are three sorts of subdivisions based on the length of the Street canyon (L).

2.1.1.4 Short canyon: (L/H) is approximately 3

2.1.1.5 Medium canyon: (L/H) is approximately 5

2.1.1.6 The length of the canyon (L/H) is approximately 7

They may be classified into two groups based on the symmetry of the canyon.

2.1.1.7 Symmetric canyon: The buildings on both sides of the road are the same height.

2.1.1.8 Asymmetric canyon: The buildings on both sides of the road are different in height.

and another category is

2.1.1.9 The Step-up Canyon: The height of the building on the upwind is less than the height of the structure on the downwind

2.2 Navier-Stokes Equations

Navier-Stokes Equations is a mathematical equation named after its developers, Claude-Louis Navier, and George Gabriel Stokes. It's a term that describes the movement of a fluid. Using the second law of Newton, Navier-Stokes The equations demonstrate momentum conservation and fluid mass conservation. It is occasionally accompanied by equations relating to temperature, pressure, and density (McLean, 2012). This can describe the flow inside a fluid tube, the flow of air around an aircraft's wings, weather simulations, etc. Equations are a set of differential equations. Theoretically, these flow problems can be solved by calculus. However, in practice, these flow equations are difficult to evaluate. As a result, computers are applied to overcome these flow equations. Also known as Computational Fluid Dynamics (CFD).

2.2.1 Equation

2.2.1.1 Conservation of mass

The mass conservation is the rate of mass accumulation in volume V is balanced by the rate of mass flux across its boundary; it is expressed as

$$\frac{\partial}{\partial t} \int \rho dV + \int \rho n \cdot u dS = 0 \quad (1)$$

Where ρ is the fluid density and u is the fluid velocity vector. The surface integral in Eq. (1) can be converted to volume integral by Gauss' divergence theorem, Thus Eq. (1) can be written as

$$\int \left[\frac{\partial}{\partial t} + \nabla \cdot (\rho u) \right] dV = 0 \quad (2)$$

Which gives the integral form, assume continuously. Since V is arbitrary, we must have

$$\frac{\partial \rho}{\partial t} + \nabla \cdot (\rho u) = 0 \quad (3)$$

By simple vector analysis, Eq. (3) can be written as

$$\frac{D\rho}{Dt} + \rho \nabla \cdot u = 0 \quad (4)$$

If the fluid is an incompressible fluid, the density ρ is constant, thus $\frac{D\rho}{Dt} = 0$ and $\nabla \cdot u = 0$

2.2.1.2 Conservation of momentum

The momentum conservation is the rate of momentum accumulation in volume V plus the flux of momentum out through S is equal to the rate of gain of momentum due to body forces and surface stresses. it is expressed as

$$\frac{\partial}{\partial t} \int \rho dV + \int \rho (n \cdot u) u dS = \int \rho f dV + \int n \cdot \sigma dS \quad (5)$$

Where f is the body force and σ is the stress tensor. Using Gauss' divergence theorem, Eq. (5) can be written as

$$\int \left[\frac{\partial}{\partial t}(\rho u) + \nabla \cdot (\rho u u) \right] dV = \int (\rho f + \nabla \cdot \sigma) dV \quad (6)$$

Where uu stands for the tensor product. V is arbitrary again, Thus

$$\frac{\partial}{\partial t}(\rho u) + \nabla \cdot (\rho u u) = \rho f + \nabla \cdot \sigma \quad (7)$$

And by vector analysis

$$u \frac{\partial \rho}{\partial t} + \rho \frac{\partial u}{\partial t} + \rho u \cdot \nabla u + u \nabla \cdot (\rho u) = \rho f + \nabla \cdot \sigma \quad (8)$$

Continuity Eq. (3) implies that the first and last terms on the left side of Eq. (8), Thus

$$\rho \frac{\partial u}{\partial t} + (\rho u) \cdot \nabla u = \rho f + \nabla \cdot \sigma \quad (9)$$

Or term of derivative,

$$\rho \frac{Du}{Dt} = \rho f + \nabla \cdot \sigma \quad (10)$$

Eq. (9) and (10) are the equation of motion

For Newtonian fluids, the relationship for the stress tensor σ is given by Newton's law as

$$\begin{cases} \sigma = -pI + \tau \\ \tau = \lambda(\nabla \cdot u)I + 2\mu D(u) \end{cases} \quad (11)$$

Where τ is the deviatoric stress tensor, $D(u) = \frac{1}{2}[\nabla u + \nabla u^T]$ is the rate of the strain tensor, p is pressure, μ is dynamic viscosity, and λ is the second coefficient of viscosity.

Instead, Eq. (11) into Eq. (10)

$$\rho \frac{Du}{Dt} = \rho f - \nabla p + \mu \Delta u + (\lambda + \mu) \nabla (\nabla \cdot u) + (\nabla \cdot u) \nabla \lambda + 2D(u) \cdot \nabla \mu \quad (12)$$

In the case of an incompressible fluid with constant viscosity, the equation of motion reduces to

$$\frac{\partial u}{\partial t} + u \cdot \nabla u = -\frac{1}{\rho} \Delta P + \nu \Delta u + f \quad (13)$$

Where $\nu = \frac{\mu}{\rho}$ is kinetic viscosity

2.2.1.3 Conservation of energy

The conservation of energy is the rate of energy accumulation in a volume V plus the flux of energy out through S is equal to the flux of heat in through S plus the rate of gain of energy due to surface stresses (dissipation). It is expressed as

$$\frac{\partial}{\partial t} \int \rho E dV + \int \rho E (n \cdot u) dS = \int n \cdot q dS + \int n \cdot (\sigma \cdot u) dS \quad (14)$$

q is the heat flux vector and E is the total energy given by

$$E = e + \frac{1}{2} u^2 - f \cdot u \quad (15)$$

Where e is internal energy, $\frac{1}{2} u^2$ is kinetic energy, and $-f \cdot u$ is potential energy. By using Gauss' divergence theorem, we have

$$\int \left[\frac{\partial}{\partial t} (\rho E) + \nabla \cdot (\rho E u) \right] dV = \int (-\nabla \cdot q + \nabla \cdot (\sigma \cdot u)) dV \quad (16)$$

V is arbitrary, Thus

$$\frac{\partial}{\partial t} (\rho E) + \nabla \cdot (\rho E u) = -\nabla \cdot q + \nabla \cdot (\sigma \cdot u) \quad (17)$$

2.3 Standard k-epsilon turbulence model

The standard k-epsilon turbulence model is a Computational fluid dynamics (CFD) model that is used to simulate flow characteristics under turbulent flow situations. It is a model that is described by two equations.

2.3.1 Turbulent kinetic energy (k)

$$\frac{\partial}{\partial t}(\rho k) + \frac{\partial}{\partial x_i}(\rho k u_i) = \frac{\partial}{\partial x_j} \left[\left(\mu + \frac{\mu_t}{\sigma_k} \right) \frac{\partial k}{\partial x_j} \right] + G_k + G_b - \rho \varepsilon \quad (18)$$

2.3.2 Rate of dissipation of turbulent kinetic energy (ε)

$$\frac{\partial}{\partial t}(\rho \varepsilon) + \frac{\partial}{\partial x_i}(\rho \varepsilon u_i) = \frac{\partial}{\partial x_j} \left[\left(\mu + \frac{\mu_t}{\sigma_\varepsilon} \right) \frac{\partial \varepsilon}{\partial x_j} \right] + C_{1\varepsilon} \frac{\varepsilon}{k} (G_k + C_{3\varepsilon} G_b) - C_{2\varepsilon} \rho \frac{\varepsilon^2}{k} \quad (19)$$

2.3.3 The turbulent (or eddy) viscosity (μ_t)

$$\mu_t = \rho C_\mu \frac{k^2}{\varepsilon} \quad (20)$$

where G_k is the generation of turbulence due to the mean velocity gradients.

G_b is the generation of turbulence due to buoyancy.

$$C_{1\varepsilon} = 1.44, \quad C_{2\varepsilon} = 1.92, \quad C_\mu = 0.09,$$

$$\sigma_k = 1.00, \quad \sigma_\varepsilon = 1.30 \quad \text{and} \quad C_{3\varepsilon} = \tanh \left| \frac{v}{u} \right|$$

σ_k and σ_ε are the turbulent Prandtl numbers for k and ε , respectively.

v is the component of the flow velocity parallel to the gravitational vector

u_i is the component of the flow velocity perpendicular to the gravitational vector.

2.4 Discrete Phase Model

ANSYS FLUENT predicts the trajectory of a discrete phase particle by integrating the particle's force balance in a Lagrangian reference frame (ANSYS, 2003). This force balance equals the particle inertia with the forces exerted on the particle, which may be expressed

$$m_p \frac{du_p}{dt} = m_p \frac{u-u_p}{\tau_r} + m_p \frac{g(\rho_p-\rho)}{\rho_p} + F \quad (21)$$

Where m_p is the particle mass, u_p is the particle velocity, ρ_p is the density of the particle, F is an addition force, and τ_r is the particle relaxation time calculated by:

$$\tau_r = \frac{\rho_p d_p^2}{18\mu} \frac{24}{C_d Re} \quad (22)$$

Where d_p is the particle diameter, and Re is the relative Reynolds number, which defined as:

$$Re \equiv \frac{\rho d_p |u_p - u|}{\mu} \quad (23)$$

Small particles suspended in a gas that has a temperature gradient, F will be define as:

$$F = -D_{T,p} \frac{1}{T} \nabla T \quad (24)$$

Where $D_{T,p}$ is the thermophoretic coefficient, which use the form suggested by Talbot (Talbot et al., 2006):

$$D_{T,p} = \frac{6\pi d_p \mu^2 C_s (K + C_t Kn)}{\rho (1 + 3C_m Kn) (1 + 2K + 2C_t Kn)} \quad (25)$$

Where Kn is Knudsen number = $2\lambda/d_p$

λ is mean free path of the fluid

K is k/k_p

k is fluid thermal conductivity based on translational energy only =

(15/4) μR

k_p is particle thermal conductivity

$C_s, C_t,$ and C_m are 1.17, 2.18, and 1.14 respectively

T is local fluid temperature

When the flow is turbulent, ANSYS FLUENT will predict the trajectories using the mean fluid velocity (\bar{u}) which express as:

$$u = \bar{u} + u' \quad (26)$$

Where u' is velocity fluctuation, which defined as:

$$u' = \zeta \sqrt{u'^2} \quad (27)$$

Where ζ is an normally distributed random number, for the k-epsilon model

$$\sqrt{u'^2} = \sqrt{2k/3} \quad (28)$$

2.5 Literature Reviews

(Walaipan.Y, 2018) The researchers investigated the effect of vehicle intake on $PM_{2.5}$ pollutants in this study. Pathumwan and Yaowarat were the two regions investigated. The Personal Modular Impactor (PMI) was used to monitor $PM_{2.5}$ concentrations, and video recording was used to record vehicle volume. Then, a linear correlation was determined by using the SSPS program. Consequently, while using the data to determine the correlation between the number of vehicles and the concentration of $PM_{2.5}$, it was observed that the Pathumwan area was near one, indicating that the number of vehicles was closely connected to the concentration of $PM_{2.5}$.

(Hao Zhang et al., 2015) The researchers investigated the parameters influencing vehicle emissions as well as the influence of wind speed on airflow and $PM_{2.5}$ concentration in this study. The simulation was performed using the Standard k- ϵ model. The incoming wind direction was perpendicular to the road and categorizes the building's form into two types:

1. Ascending type model of street canyon

Ascending Street Canyon's result, according to the airflow characteristics, if the windward building was higher than the leeward building, the flowing air would hit the windward building wall and fall to produce a clockwise vortex. The vortex becomes more intense as the wind speed increases. The parameters of air pollution diffusion since the wind flows clockwise in the canyon, it blows $PM_{2.5}$ from the leeward side, causing the $PM_{2.5}$ concentration to be higher on the leeward side than on the windward side.

2. Decreasing type model of street canyon

Because the height of the leeward side is higher than the windward side. The air flows up the building and descends to produce a clockwise vortex at the top. When the wind blows against the building's leeward side, it flows down, forming a counterclockwise vortex inside the canyon. Because of the vortex in different directions. $PM_{2.5}$ dispersion in the canyon is blown to the windward side, resulting in a higher $PM_{2.5}$ concentration on the windward side than on the leeward side.

(Narut Sahanavin et al., 2016) The research investigated the dispersion of PM_{10} and $PM_{2.5}$ in two different structural regions in this study. The research area is divided into two areas: On Asoke Montri Road, there is an open area. The second area is the covered area, which is surrounded by sky trains on Sukhumvit Road. A total of eight samples were collected, each of which represented a different aspect ratio. The PM_{10} and $PM_{2.5}$ sampling equipment will be installed at a roadside traffic sign at 1.6 meters in height, representing the location of human breathing, and 1 meter away from the road's edge. The samples were taken at two different times: 5 AM to 1 PM and 1 PM to 9 PM Meteorological data is collected at a height of 3 meters. The relationship between PM_{10} and $PM_{2.5}$ is correlated with meteorological data. The results revealed that as the aspect ratio was increased in the open area, the PM_{10} and

PM_{2.5} levels increased. When 5 AM to 1 PM was compared to 1 PM to 9 PM, PM₁₀ and PM_{2.5} levels were higher. When investigating the relationship between the values of PM₁₀ and PM_{2.5} and the influencing factor. It was discovered that the open area's wind speed and relative humidity were negative, whereas the covered area was positive. In the covered area, the temperature was negative with PM₁₀ and PM_{2.5} but positive in the open area. There is a positive relationship between PM₁₀ and PM_{2.5}.

(Daniel(Jian) Sun & Zhang, 2018) The researchers investigated the effects of roadside trees in Street Canyon in their study. The simulation was performed using the Standard k- ϵ model. When the influence of wind direction is considered, results have been obtained. When the wind blows from the southeast or right, a vortex forms in region M (the windward side), which is counterclockwise, and area N (the leeward side), which is clockwise. When the wind blows from the north-west or the left, a vortex forms in areas K (the windward side) and J (the leeward side), which are clockwise and counterclockwise, respectively. When the wind blows from the southeast or the right, the impact of the tree is considered. Scenario A (having a tree) had lower pollutant concentrations than Scenario B (no tree). However, due to the presence of trees, air pollution on the windward side was higher in Area M than in Area N. The airflow in area N is decreased, as is the air exchange between the two zones. Pollutants accumulate in region N when the wind blows from the north or the left. When roadside trees were planted in scenario C (having a tree), the pollutant concentration in region J was greater than in scenario D (no tree). The significant increase in pollution over the surface A and around trees is due to high wind speeds between trees. Wind currents carry pollutants to accumulate within the area.

(Jandaghian, 2018) In this research, the researcher studied the ethane gas flow characteristics in Urban Street Canyon, wind speed, and temperature

using three models: standard k-epsilon, RNG k-epsilon, and realizable k-epsilon. In comparison to the calculated data, the simulation results showed that the RNG k-epsilon model was the most suitable. As well as the ethane gas concentration on the leeward side, there will be huge value.



Chapter 3

Methodology

The investigation of $PM_{2.5}$ dispersion in Din Daeng district, Bangkok using Computational Fluid Dynamics modeling aims to study the dispersion of $PM_{2.5}$ using Ansys Fluent 19.2. As shown in Table 1-3, which is the $PM_{2.5}$ data in the Din Daeng area in 2019–2021 (P. C. Department, 2019-2021a), it is one of the areas where the $PM_{2.5}$ level exceeds the standard. After that, explore a guideline solution to lower $PM_{2.5}$ concentrations. The process is divided into 3 steps as follows.

3.1 Preparing the necessary information

3.2 Study area

3.3 Model Simulation

Table 1: $PM_{2.5}$ values in the area along Din Daeng Road, Din Daeng District, 2019.

2019			
Month	$PM_{2.5}$		monthly average
	24-hour average		
	Maximum	Minimum	
January	91	30	58
February	67	15	32
March	46	21	32
April	49	17	29
May	45	17	30
June	35	16	24
July	35	13	25
August	28	15	20
September	83	18	32
October	58	25	34
November	58	23	40

December	59	21	44
annual average			33

Table 2: PM_{2.5} values in the area along Din Daeng Road, Din Daeng District, 2020.

2020			
Month	PM _{2.5}		monthly average
	24-hour average		
	Maximum	Minimum	
January	102	23	52
February	87	22	50
March	53	23	32
April	50	21	30
May	37	15	26
June	25	17	21
July	24	14	21
August	28	13	20
September	37	18	22
October	53	18	28
November	54	24	37
December	112	22	47
annual average			32

Table 3: PM_{2.5} values in the area along Din Daeng Road, Din Daeng District, 2021.

2021			
Month	PM _{2.5}		monthly average
	24-hour average		
	Maximum	Maximum	
January	106	24	53
February	78	39	57

March	58	26	40
April	61	13	32
May	35	16	24
June	31	17	23
July	33	14	21
August	27	15	20
September	43	17	24
October	46	14	27
November	43	22	31
December	75	23	41
annual average			33

According to Table 1-3, shows the concentration of $PM_{2.5}$ from 2019 - 2021, at the beginning of the year (January to April) and at the end of the year (October to December). There were an average $PM_{2.5}$ value of 24 hours that exceeded Thailand's national air quality standard (over 50 micrograms/cubic meter) and during the years 2019 - 2021, the average annual $PM_{2.5}$ value exceeded Thailand's national air quality standard as well (over 25 micrograms/cubic meter) (Pollution Control Department, 2018). As can be observed, January has a higher $PM_{2.5}$ value than any other month, so the January data was selected for simulation in this study.

3.1 Preparing the necessary information

Temperature, wind speed, wind direction, city planning, and traffic volume were all employed in the simulation. Table 4 shows data obtained from government entities.

Table 4: Data for simulations and sources.

Data	Source
Geographical data (City plan)	Department of City Planning and Urban Development, BMA
Meteorological data	Pollution Control Department
Traffic volume (Emission source)	Traffic and Transportation Department and Expressway Authority of Thailand
PM _{2.5} data	Air Quality and Noise Management Division Bangkok

The simulation is divided into 2 scenarios:

3.1.1 Simulation with and without the COVID-19 pandemic.

During the absence of the COVID-19 pandemic, the simulation employed meteorological data, traffic volume data, and PM_{2.5} concentration data from January 27, 2020, which were compared to simulated results from the COVID-19 pandemic. Using data from January 25, 2021, to compare how the outcomes differ.

3.1.2 Simulation with and without expressways.

The presence of expressways in the area results in more traffic flowing through the area. Therefore, in this study, the effect of the presence and absence of expressways on how they affect the concentration of PM_{2.5} is studied.

3.2 Study area

The investigation was carried out in the Din Daeng District, one of Bangkok's 50 districts. It has an area of 8.354 square kilometers. and has a population of about 112,814 people ((BORA), 2020). It is a densely populated area consisting of residential

buildings, government offices, educational institutions, and commercial areas. Din Daeng's overall area is composed of buildings that are not particularly tall. However, the building density is high, and the streets are relatively narrow. The studied area is approximately 2 square kilometers, covering Bangkok's air quality monitoring station (b56). There are three main roads: Din Daeng, Pracha Songkhro, and Mitmaitri Roads, as well as two expressways: Chalem Mahanakorn and Si Rat Expressways. The focused area is shown in Figure 2.



Figure 2: Focused area for the investigation of $PM_{2.5}$ dispersion in Din Daeng.

3.3 Model Simulation

3.3.1 Geometric Model

The study area is approximately 2 square kilometers. By using data from the Department of City Planning and Urban Development, BMA, which is geographic and urban planning data, to create geometry in the Ansys SpaceClaim, build 3 main roads for use as emission sources (Daniel(Jian) Sun & Zhang, 2018), namely Din Daeng Road, Pracha Songkhro Road, and Mitmaitri Road. Geometry will be obtained as shown in Figure 3. The expressway will be 25 meters wide and 14 meters high, with the size of the pillars at 2.1 meters

wide and 1.2 meters thick (SUPERSTRUCTURE RAILWAY OF BANGKOK, 2017), as shown in Figure 4.



Figure 3: Geometry of the focused area.

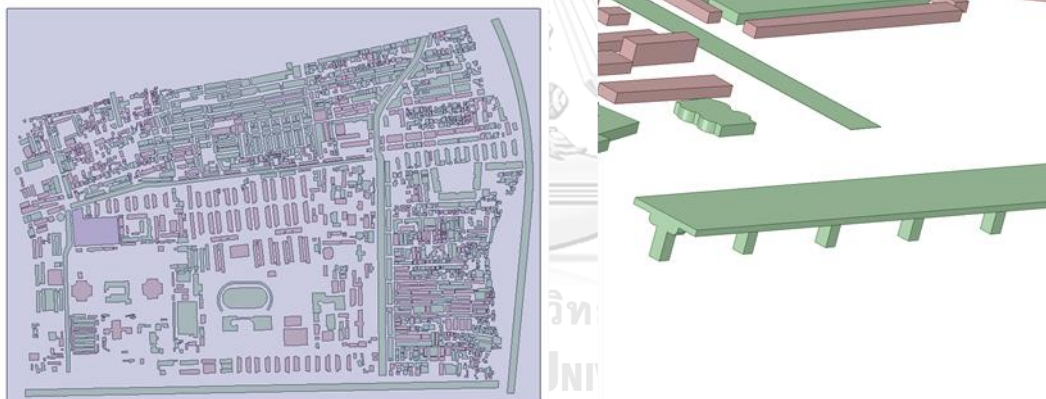


Figure 4: Structure of expressway.

3.3.2 Computational domain

Based on the study by (Eric R. Pardyjak, 2001), the distance at which the building had no effect on the velocity profile was equivalent to 1.25 times the height of the tallest building on that side (H_{max}). In this study, the upper and lateral boundaries are 1.25 times H_{max} . The computational domain is as shown in Figure 5.

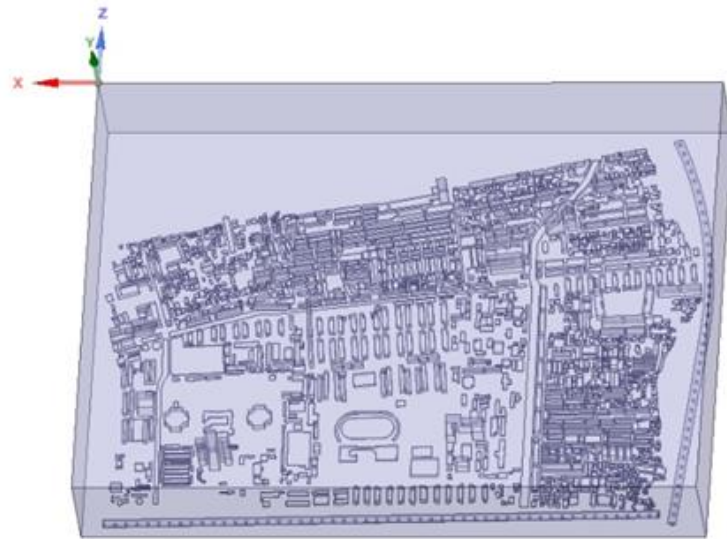


Figure 5: Computational domain of the focused area.

3.3.3 Generic mesh

Following the progress of the computational domain, the next step will be the generation of mesh, which is divided into

- The generation of mesh for the whole domain is shown in Table 5.

Table 5: Details of mesh.

Defaults	
Physics Preference	CFD
Solver Preference	Fluent
Element Order	Linear
- Element Size	15.0 m
Export Format	Standard
Export Preview Surface Mesh	No
Sizing	
Use Adaptive Sizing	No
- Growth Rate	Default (1.2)
- Max Size	Default (30.0 m)
Mesh Defeaturing	Yes
- Defeature Size	Default (7.5e-002 m)

Capture Curvature	Yes
- Curvature Min Size	Default (0.15 m)
- Curvature Normal Angle	Default (18.0°)
Capture Proximity	No
Bounding Box Diagonal	10,834 m
Average Surface Area	908.88 m ³
Minimum Edge Length	1.5778e-003 m
Quality	
Check Mesh Quality	Yes, Errors
- Target Skewness	Default (0.9)
Smoothing	Medium
Inflation	
Use Automatic inflation	None
Inflation Option	Smooth Transition
- Transition Ratio	0.272
- Maximum Layers	5
- Growth Rate 1.2	
Inflation Algorithm	Pre
View Advanced Options	No
Assembly Meshing	
Method	None
Advanced	
Number of CPUs for Parallel Part Meshing	Program Controlled
Straight Sided Elements	
Rigid Body Behavior	Dimensionally Reduced
Triangle Surface Mesher	Program Controlled
Topology Checking	Yes
Pinch Tolerance	Default (0.135 m)
Generate Pinch on Refresh	No

- The generation of mesh around the four edges of the domain is shown in Table 6.

Table 6: Detail of mesh on four edges of the domain.

Definition	
Suppressed	No
Type	Element Size
- Element Size	15.0 m
Advanced	
Behavior	Soft
- Growth Rate	Default (1.2)
Capture Curvature	No
Capture Proximity	No
Bias Type	No Bias

- The generation of mesh on the three roads is shown in Table 7.

Table 7: Detail of mesh in the three roads.

Definition	
Suppressed	No
Type	Element Size
- Element Size	3.5 m
Advanced	
Behavior	Soft
- Growth Rate	Default (1.2)
Capture Curvature	No
Capture Proximity	No
Bias Type	No Bias

- The generation of mesh residence building area It is shown in Table 8.

Table 8: Detail of mesh in the residence building area.

Definition	
Suppressed	No
Type	Element Size
- Element Size	5.0 m
Advanced	
- Defeature Size	Default (7.5e-002 m)
- Growth Rate	Default (1.2)
Capture Curvature	No
Capture Proximity	No

- The generation of mesh around both expressway lines is shown in Table 9.

Table 9: Detail of mesh around both expressway lines.

Definition	
Suppressed	No
Type	Element Size
- Element Size	5.0 m
Advanced	
- Defeature Size	Default (7.5e-002 m)
- Growth Rate	Default (1.2)
Capture Curvature	No
Capture Proximity	No

After determining the size of the mesh, it can generate the mesh as shown in Figure 6 and 7. The effect of the mesh quality and the number of meshes can be divided into

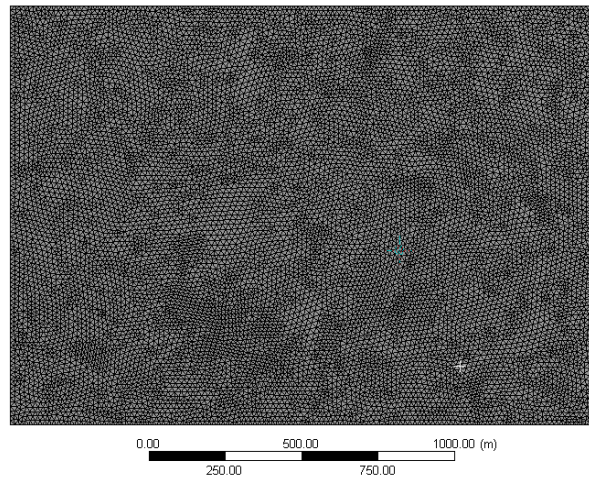


Figure 6: Mesh of CFD simulation (front view).

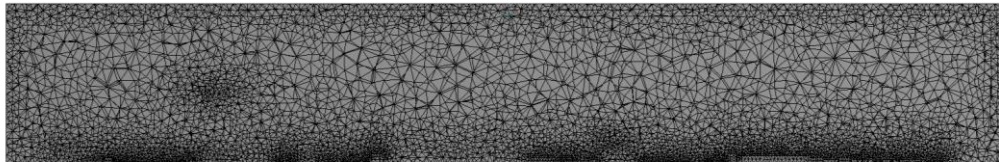


Figure 7: Mesh of CFD simulation (side view).

- The quality and amount of mesh in the case of the expressways are shown in Table 10.

Table 10: The quality and amount of mesh in the case of the expressways.

Quality	
Mesh Metric	Element Quality
Min	6.9429e-002
Max	0.99997
Average	0.82607
Standard Deviation	0.10345
Mesh Metric	Aspect Ratio
Min	1.1597
Max	44.71

Average	1.8848
Standard Deviation	0.51311
Mesh Metric	Skewness
Min	6.3508e-005
Max	0.98972
Average	0.24417
Standard Deviation	0.13136
Mesh Metric	Orthogonal quality
Min	1.0277e-002
Max	0.99639
Average	0.75451
Standard Deviation	0.12969
Statistics	
Nodes	714,609
Elements	3,783,145

- The quality and amount of mesh in the case of no expressways is shown in Table 11.

Table 11: The quality and amount of mesh in the case of no expressways.

Quality	
Mesh Metric	Element Quality
Min	8.4554e-002
Max	0.99999
Average	0.82646
Standard Deviation	0.10323
Mesh Metric	Aspect Ratio
Min	1.1598
Max	23.148
Average	1.8838
Standard Deviation	0.512

Mesh Metric	Skewness
Min	1.0019e-005
Max	0.98972
Average	0.24348
Standard Deviation	0.13085
Mesh Metric	Orthogonal quality
Min	1.0277e-002
Max	0.99501
Average	0.7552
Standard Deviation	0.12918
Statistics	
Nodes	661,778
Elements	3,500,401

3.3.4 Setup

The default setup setting defines Fluent Launcher (Setting Edit Only) as shown in Figure 8. Then set the equation model and the model that will be used to simulate PM_{2.5} dispersion. Initially, Setup General by defining Solver as shown in Figure 9 and specifying Gravitational Acceleration as shown in Figure 10, then specifying the model of the model by Energy Model set to On, Viscous Model as Standard k - ϵ , Standard Wall. The constant values shown in Table 12 and using the Discrete Phase Model set to On, then setting the Injections section in the simulation to PM_{2.5} emitted from the road and having carbon as the main component (Krerkkaiwal, 2000)

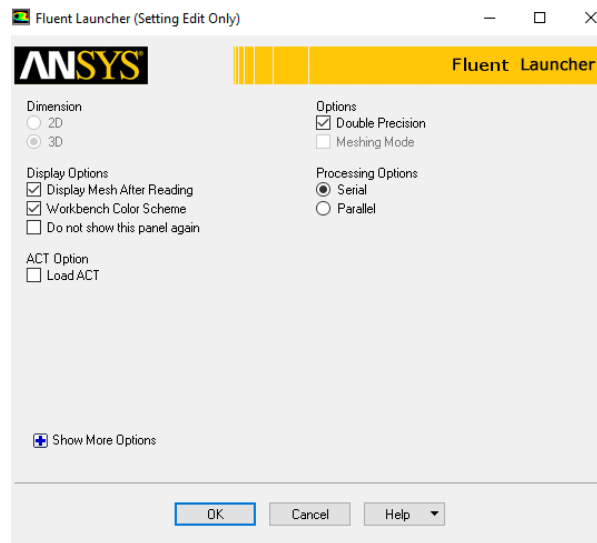


Figure 8: Setting Fluent Launcher (Setting Edit Only).

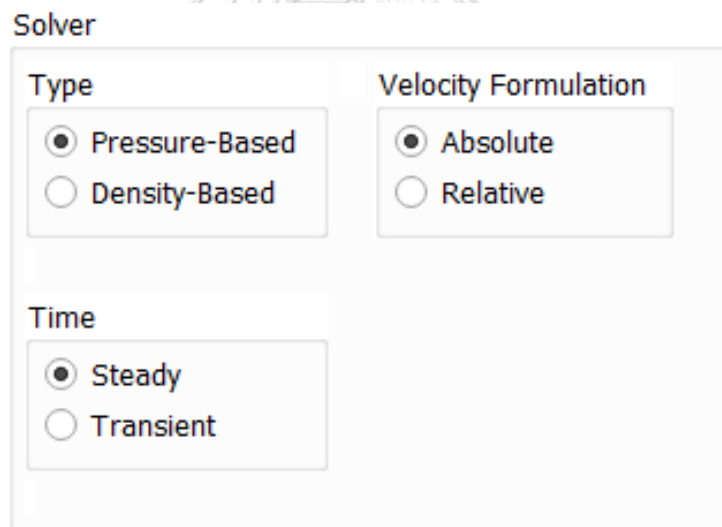


Figure 9: Setting Solver.

Gravitational Acceleration

X (m/s ²)	0	P
Y (m/s ²)	0	P
Z (m/s ²)	-9.81	P

Figure 10: Gravitational Acceleration.

Because $PM_{2.5}$ is emitted from the road surface, set the Injection Type to the surface, which is released from the road surface, set the Particle Type to Inert Material, and set the Diameter to $2.5E-06$ because that is the diameter of the carbon. The temperature is set to the temperature of the road, which is equal to the air temperature in the study period plus 13 (Y. Nakamura & Oke, 1988) as shown in Figure 11.

Table 12: Constants used in the Standard $k-\epsilon$ Model.

Model Constants	
Cmu	0.09
C1-Epsilon	1.44
C2-Epsilon	1.92
TKE Prandtl Number	1
TDR Prandtl Number	1.3
Energy Prandtl Number	0.85
Wall Prandtl Number	0.85

Set Injection Properties

Injection Name: injection-ce Injection Type: surface

Highlight Surfaces

Release From Surfaces: Filter Text

- c-express
- d_road
- ground
- inlet
- interior
- m_road
- outlet
- p_road
- plane-13

Particle Type: Massless Inert Droplet Combusting Multicomponent Laws: Custom

Material: carbon Diameter Distribution: uniform Oxidizing Species: none Discrete Phase Domain: none

Evaporating Species: Devolatilizing Species: Product Species:

Point Properties Physical Models Turbulent Dispersion Parcel Wet Combustion Components UDF Multiple Reactions

Variable	Value
Diameter (m)	2.5e-06
Temperature (k)	313.5167
Velocity Magnitude (m/s)	0
Total Flow Rate (kg/s)	1.18e-06

Stagger Options: Stagger Positions Stagger Radius (m): 0

Scale Flow Rate by Face Area Inject Using Face Normal Direction

OK File... Cancel Help

Figure 11: Setting injections.

The simulation of PM_{2.5} dispersion is divided into 3 periods of time: 7 AM - 9 AM, 10 AM - 12 PM, and 1 PM - 4 PM. Equation 29 (X. Xie et al., 2005) can be used to calculate the total flow rate.

$$\text{Mass Flow Rate} = \frac{\sum Q_i \cdot f_i \cdot l}{3600} \quad (29)$$

where Q_i is the traffic volume of a type i motor vehicle (veh/h), f_i is the Emission factor of the type i motor vehicle (kg/km·veh) and l is the length of the road (km). Emission factor for each vehicle type and the lengths of roads and expressways in the model are shown in Tables 13 and 14, respectively.

Table 13: Emission factor for each vehicle type. (EMEP/EEA, 2006)

Vehicle type	Emission factor (g/km)
Two-wheeler	0.0035
Three-wheeler	0.0114
Passenger car	0.0011
Heavy commercial vehicles	0.0783
Bus	0.0354

Table 14: The lengths of roads and expressways in the model.

Road and Expressway Name	Length (km)
Din Daeng road	1.3000
Pracha Songkhro road	1.1180
Mitmaitri Roads	0.5961
Chalerm Mahanakorn expressway	1.7345
Si Rat expressway	1.3868

In the calculation during the non-affected period of COVID-19, the traffic volume data of January 27, 2020, obtained from the Traffic and Transportation Department, will be calculated using equation (29) to calculate.

- 7 AM – 9 AM

Table 15: Traffic volume from 7 AM – 9 AM around Din Daeng Road and Traffic volume from 6:30 AM - 9 AM on Pracha Songkhro and Mitmaitri Roads during normal period.

Roads	Vehicle type (vehicle)					
	Passenger car	Van/Pick-up	Big bus	Small bus	Truck	Three-wheeler
Din Daeng	5,101	1,105	181	30	12	5
Pracha Songkhro	477	135	49	24	8	72
Mitmaitri	1,226	301	110	26	13	65

Emission Rate of Din Daeng rd.

$$= \left[\left(\frac{5101 + 1105}{2} \times 0.0011 \times 10^{-3} \right) + \left(\frac{181 + 30}{2} \times 0.0354 \times 10^{-3} \right) + \left(\frac{12}{2} \times 0.0783 \times 10^{-3} \right) + \left(\frac{5}{2} \times 0.0114 \times 10^{-3} \right) \right] \times \frac{1.3}{3600}$$

Emission Rate of Din Daeng rd. = 2.76274E – 06 kg/s (Per 1 hour)

Between 7 AM - 9 AM there are 2 hours.

Emission Rate of Din Daeng = 5.52549E – 06 kg/s

Emission Rate of Pracha Songkhro rd.

$$= \left[\left(\frac{477+135}{2} \times 0.0011 \times 10^{-3} \right) + \left(\frac{49+24}{2} \times 0.0354 \times 10^{-3} \right) + \left(\frac{8}{2} \times 0.0783 \times 10^{-3} \right) + \left(\frac{72}{2} \times 0.0114 \times 10^{-3} \right) \right] \times \frac{1.118}{3600}$$

Emission Rate of Pracha Songkhro rd. = 5.80377 – 06 kg/s (Per 1 hour)

Between 7 AM - 9 AM there are 2 hours.

Emission Rate of Pracha Songkhro rd. = 1.16075E – 06 kg/s

Emission Rate of Mitmaitri rd.

$$= \left[\left(\frac{1226 + 301}{2.5} \times 0.0011 \times 10^{-3} \right) + \left(\frac{110 + 26}{2.5} \times 0.0354 \times 10^{-3} \right) + \left(\frac{13}{2.5} \times 0.0783 \times 10^{-3} \right) + \left(\frac{65}{2.5} \times 0.0114 \times 10^{-3} \right) \right] \times \frac{0.5961}{3600}$$

Emission Rate of Mitmaitri rd. = 5.46622E – 07 kg/s (Per 1 hour)

Between 7 AM - 9 AM there are 2 hours.

Emission Rate of Mitmaitri rd. = 1.0932E – 06 kg/s

Note: Due to the amount of traffic on Pracha Songkhro and Mitmaitri Roads, it is Traffic volume between 6:30 AM and 9 AM, so divide by 2.5 hours.

- 10 AM -12 PM

Table 16: Traffic volume from 9 AM – 4 PM around Din Daeng, Pracha Songkhro, and Mitmaitri Roads during the normal period.

Roads	Vehicle type (vehicle)					
	Passenger car	Van/Pick-up	Big bus	Small bus	Truck	Three-wheeler
Din Daeng	13,244	4,069	598	60	167	88
Pracha Songkhro	1,338	726	239	72	44	232
Mitmaitri	4,239	1,262	345	82	70	229

Emission Rate of Din Daeng rd.

$$= \left[\left((13244 + 4069) \times \frac{2}{7} \times 0.0011 \times 10^{-3} \right) + \left((598 + 60) \times \frac{2}{7} \times 0.0354 \times 10^{-3} \right) + \left(167 \times \frac{2}{7} \times 0.0783 \times 10^{-3} \right) + \left(88 \times \frac{2}{7} \times 0.0114 \times 10^{-3} \right) \right] \times \frac{1.3}{3600}$$

Emission Rate of Din Daeng rd. = 5.82E – 06 kg/s (Per 2 hours)

Emission Rate of Pracha Songkhro rd.

$$= \left[\left((1338 + 726) \times \frac{2}{7} \times 0.0011 \times 10^{-3} \right) + \left((239 + 72) \times \frac{2}{7} \times 0.0354 \times 10^{-3} \right) + \left(44 \times \frac{2}{7} \times 0.0783 \times 10^{-3} \right) + \left(232 \times \frac{2}{7} \times 0.0114 \times 10^{-3} \right) \right] \times \frac{1.118}{3600}$$

Emission Rate of Pracha Songkhro rd. = 1.72E – 06 kg/s (Per 2 hours)

Emission Rate of Mitmaitri rd.

$$= \left[\left((4239 + 1262) \times \frac{2}{7} \times 0.0011 \times 10^{-3} \right) + \left((345 + 82) \times \frac{2}{7} \times 0.0354 \times 10^{-3} \right) + \left(70 \times \frac{2}{7} \times 0.0783 \times 10^{-3} \right) + \left(229 \times \frac{2}{7} \times 0.0114 \times 10^{-3} \right) \right] \times \frac{0.596}{3600}$$

Emission Rate of Mitmaitri rd. = 1.38E – 06 kg/s (Per 2 hours)

- 1 PM – 4 PM

Emission Rate of Din Daeng rd.

$$= \left[\left((13244 + 4069) \times \frac{3}{7} \times 0.0011 \times 10^{-3} \right) + \left((598 + 60) \times \frac{3}{7} \times 0.0354 \times 10^{-3} \right) + \left(167 \times \frac{3}{7} \times 0.0783 \times 10^{-3} \right) + \left(88 \times \frac{3}{7} \times 0.0114 \times 10^{-3} \right) \right] \times \frac{1.3}{3600}$$

Emission Rate of Din Daeng rd. = 8.74E – 06 kg/s (Per 3 hours)

Emission Rate of Pracha Songkhro rd.

$$= \left[\left((1338 + 726) \times \frac{3}{7} \times 0.0011 \times 10^{-3} \right) + \left((239 + 72) \times \frac{3}{7} \times 0.0354 \times 10^{-3} \right) + \left(44 \times \frac{3}{7} \times 0.0783 \times 10^{-3} \right) + \left(232 \times \frac{3}{7} \times 0.0114 \times 10^{-3} \right) \right] \times \frac{1.118}{3600}$$

Emission Rate of Pracha Songkhro rd. = 2.58 – 06 kg/s (Per 3 hours)

Emission Rate of Mitmaitri rd.

$$= \left[\left((4239 + 1262) \times \frac{3}{7} \times 0.0011 \times 10^{-3} \right) + \left((345 + 82) \times \frac{3}{7} \times 0.0354 \times 10^{-3} \right) + \left(70 \times \frac{3}{7} \times 0.0783 \times 10^{-3} \right) + \left(229 \times \frac{3}{7} \times 0.0114 \times 10^{-3} \right) \right] \times \frac{0.596}{3600}$$

Emission Rate of Mitmaitri rd. = 2.08E – 06 kg/s (Per 3 hours)

The data obtained from the Thai Expressway Authority will be used to calculate the emission rate in the expressway area, as indicated in Table 17.

Table 17: Traffic Volume of the Chalerm Mahanakorn and the Si Rat Expressways during the normal period.

Traffic volume	Chalerm Mahanakorn Expressway		Si Rat Expressway	
	Passenger car	Heavy commercial vehicles	Passenger car	Heavy commercial vehicles
Traffic volume per month	248,806	7,774	3,994,503	74,182
Traffic volume per hour	346	11	5,548	103

Emission Rate of Chalerm Mahanakorn Expr.

$$= [(346 \times 0.0011 \times 10^{-3}) + (11 \times 0.0783 \times 10^{-3})] \times \frac{1.7345}{3600}$$

Emission Rate of Chalerm Mahanakorn Expr. = 5.90464E – 07 kg/s

Emission Rate of Si Rat Expr.

$$= [(5548 \times 0.0011 \times 10^{-3}) + (103 \times 0.0783 \times 10^{-3})] \times \frac{1.3868}{3600}$$

Emission Rate of Si Rat Expr. = 5.45844E – 06 kg/s

Therefore, the three time periods, which are 7 AM - 9 AM, 10 AM - 12 PM, and 1 PM - 4 PM, are equal to

- 7 AM – 9 AM

Emission Rate of Chalerm Mahanakorn Expr. = 1.18E – 06 $\frac{kg}{s}$ (Per 2 hours)

Emission Rate of Si Rat Expr. = 1.09169E – 05 kg/s

(Per 2 hours)

- 10 AM – 12 PM

$$\text{Emission Rate of Chalerm Mahanakorn Expr.} = 1.18E - 06 \frac{\text{kg}}{\text{s}} \text{ (per 2 hours)}$$

$$\text{Emission Rate of Si Rat Expr.} = 1.09169E - 05 \text{ kg/s (Per 2 hours)}$$

- 1 PM – 4 PM

$$\text{Emission Rate of Chalerm Mahanakorn Expr.} = 1.77E - 06 \frac{\text{kg}}{\text{s}} \text{ (Per 3 hours)}$$

$$\text{Emission Rate of Si Rat Expr.} = 1.63753E - 05 \text{ kg/s (Per 3 hours)}$$

Subsequently, it will be calculated during the impact of COVID-19 pandemic. In the calculation during the impact of COVID-19 pandemic, the traffic volume data on January 25, 2021, obtained from the Traffic and Transportation Department, will be calculated using the equation (29) to calculate.

- 7 AM – 9 AM

Table 18: Traffic volume from 7 AM – 9 AM around Din Daeng Road and traffic volume from 6.30 AM – 9 AM in Pracha Songkhro, and Mitmaitri Roads during the lockdown period.

Roads	Vehicle type (vehicle)					
	Passenger car	Van/Pick-up	Big bus	Small bus	Truck	Three-wheeler
Din Daeng rd.	3,181	689	113	19	7	3
Pracha Songkhro rd.	279	84	31	15	5	45
Mitmaitri rd.	765	188	69	16	8	41

Emission Rate of Din Daeng rd.

$$= \left[\left(\frac{3181 + 689}{2} \times 0.0011 \times 10^{-3} \right) + \left(\frac{113 + 19}{2} \times 0.0354 \times 10^{-3} \right) + \left(\frac{7}{2} \times 0.0783 \times 10^{-3} \right) + \left(\frac{3}{2} \times 0.0114 \times 10^{-3} \right) \right] \times \frac{1.3}{3600}$$

Emission Rate of Din Daeng rd. = 1.71845E – 06 kg/s (Per 1 hour)

Between 7 AM - 9 AM there are 2 hours.

Emission Rate of Din Daeng = 3.43689E – 06 kg/s

Emission Rate of Pracha Songkhro rd.

$$= \left[\left(\frac{279+84}{2} \times 0.0011 \times 10^{-3} \right) + \left(\frac{31+15}{2} \times 0.0354 \times 10^{-3} \right) + \left(\frac{5}{2} \times 0.0783 \times 10^{-3} \right) + \left(\frac{45}{2} \times 0.0114 \times 10^{-3} \right) \right] \times \frac{1.118}{3600}$$

Emission Rate of Pracha Songkhro rd. = 3.64282 – 07 kg/s (Per 1 hour)

Between 7 AM - 9 AM there are 2 hours.

Emission Rate of Pracha Songkhro rd. = 7.2856E – 07 kg/s

Emission Rate of Mitmaitri rd.

$$= \left[\left(\frac{765 + 188}{2.5} \times 0.0011 \times 10^{-3} \right) + \left(\frac{69 + 16}{2.5} \times 0.0354 \times 10^{-3} \right) + \left(\frac{8}{2.5} \times 0.0783 \times 10^{-3} \right) + \left(\frac{41}{2.5} \times 0.0114 \times 10^{-3} \right) \right] \times \frac{0.5961}{3600}$$

Emission Rate of Mitmaitri rd. = 3.41173E – 07 kg/s (Per 1 hour)

Between 7 AM - 9 AM there are 2 hours.

Emission Rate of Mitmaitri rd. = 6.82346E – 07 kg/s

Note: Due to the amount of traffic on Pracha Songkhro and Mitmaitri Roads. It is Traffic volume between 6:30 AM and 9 AM, so divide by 2.5 hours.

- 10 AM – 12 PM

Table 19: Traffic volume from 9 AM. – 4 PM on Din Daeng, Pracha Songkhro, and Mitmaitri Roads during the lockdown period.

Roads	Vehicle type (vehicle)					
	Passenger car	Van/Pick-up	Big bus	Small bus	Truck	Three-wheeler
Din Daeng	10,814	3,322	488	49	136	72
Pracha Songkhro	1,092	593	195	59	36	189
Mitmaitri	3,461	1,030	282	67	57	187

Emission Rate of Din Daeng rd.

$$= \left[\left((10814 + 3322) \times \frac{2}{7} \times 0.0011 \times 10^{-3} \right) + \left((488 + 49) \times \frac{2}{7} \times 0.0354 \times 10^{-3} \right) + \left(136 \times \frac{2}{7} \times 0.0783 \times 10^{-3} \right) + \left(72 \times \frac{2}{7} \times 0.0114 \times 10^{-3} \right) \right] \times \frac{1.3}{3600}$$

Emission Rate of Din Daeng rd. = 4.75E – 06 kg/s (Per 2 hours)

Emission Rate of Pracha Songkhro rd.

$$= \left[\left((1092 + 593) \times \frac{2}{7} \times 0.0011 \times 10^{-3} \right) + \left((195 + 59) \times \frac{2}{7} \times 0.0354 \times 10^{-3} \right) + \left(136 \times \frac{2}{7} \times 0.0783 \times 10^{-3} \right) + \left(72 \times \frac{2}{7} \times 0.0114 \times 10^{-3} \right) \right] \times \frac{1.118}{3600}$$

Emission Rate of Pracha Songkhro rd. = 1.40E – 06 kg/s (Per 2 hours)

Emission Rate of Mitmaitri rd.

$$= \left[\left((3461 + 1030) \times \frac{2}{7} \times 0.0011 \times 10^{-3} \right) + \left((282 + 67) \times \frac{2}{7} \times 0.0354 \times 10^{-3} \right) + \left(57 \times \frac{2}{7} \times 0.0783 \times 10^{-3} \right) + \left(187 \times \frac{2}{7} \times 0.0114 \times 10^{-3} \right) \right] \times \frac{0.596}{3600}$$

Emission Rate of Mitmaitri rd. = 1.13E – 06 kg/s (Per 2 hours)

- 1 PM – 4 PM.

Emission Rate of Din Daeng rd.

$$= \left[\left((10814 + 3322) \times \frac{3}{7} \times 0.0011 \times 10^{-3} \right) + \left((488 + 49) \times \frac{3}{7} \times 0.0354 \times 10^{-3} \right) + \left(136 \times \frac{3}{7} \times 0.0783 \times 10^{-3} \right) + \left(72 \times \frac{3}{7} \times 0.0114 \times 10^{-3} \right) \right] \times \frac{1.3}{3600}$$

Emission Rate of Din Daeng rd. = 7.13E – 06 kg/s (Per 3 hours)

Emission Rate of Pracha Songkhro rd.

$$= \left[\left((1092 + 593) \times \frac{3}{7} \times 0.0011 \times 10^{-3} \right) + \left((195 + 59) \times \frac{3}{7} \times 0.0354 \times 10^{-3} \right) + \left(136 \times \frac{3}{7} \times 0.0783 \times 10^{-3} \right) + \left(72 \times \frac{3}{7} \times 0.0114 \times 10^{-3} \right) \right] \times \frac{1.118}{3600}$$

Emission Rate of Pracha Songkhro rd. = 2.11 – 06 kg/s (Per 3 hours)

Emission Rate of Mitmaitri rd.

$$= \left[\left((3461 + 1030) \times \frac{3}{7} \times 0.0011 \times 10^{-3} \right) + \left((282 + 67) \times \frac{3}{7} \times 0.0354 \times 10^{-3} \right) + \left(57 \times \frac{3}{7} \times 0.0783 \times 10^{-3} \right) + \left(187 \times \frac{3}{7} \times 0.0114 \times 10^{-3} \right) \right] \times \frac{0.596}{3600}$$

Emission Rate of Mitmaitri rd. = 1.70E – 06 kg/s (Per 3 hours)

The data obtained from the Expressway Authority of Thailand will be used to calculate the emission rate in that expressway area, which will be calculated as stated in Table 20.

Table 20: Traffic Volume of the Chalerm Mahanakorn and the Si Rat Expressways during the lockdown period.

Traffic volume	Chalerm Mahanakorn Expressway		Si Rat Expressway	
	Passenger car	Heavy commercial vehicles	Passenger car	Heavy commercial vehicles
Traffic volume per month	204,593	6,393	3,284,671	61,000
Traffic volume per hour	284	9	4,562	85

Emission Rate of Chalerm Mahanakorn Expr.

$$= [(284 \times 0.0011 \times 10^{-3}) + (9 \times 0.0783 \times 10^{-3})] \times \frac{1.7345}{3600}$$

Emission Rate of Chalerm Mahanakorn Expr. = 4.85537E - 07 kg/s

Emission Rate of Si Rat Expr.

$$= [(4562 \times 0.0011 \times 10^{-3}) + (85 \times 0.0783 \times 10^{-3})] \times \frac{1.3868}{3600}$$

Emission Rate of Si Rat Expr. = 4.48846E - 06 kg/s

Therefore, the three time periods, which are 7 AM - 9 AM, 10 AM - 12 PM, and 1 PM - 4 PM, are equal to

- 7 AM - 9 AM

Emission Rate of Chalerm Mahanakorn Expr. = 9.71E - 07 $\frac{kg}{s}$ (Per 2 hours)

Emission Rate of Si Rat Expr. = 8.97692E - 06 $\frac{kg}{s}$

(Per 2 hours)

- 10 AM - 12 PM

Emission Rate of Chalerm Mahanakorn Expr. = 9.71E - 07 $\frac{kg}{s}$ (Per 2 hours)

Emission Rate of Si Rat Expr. = $8.97692E - 06$ kg/s (Per 2 hours)

- 1 PM – 4 PM

Emission Rate of Chalerm Mahanakorn Expr. = $1.46E - 06$ $\frac{kg}{s}$ (per 3 hours)

Emission Rate of Si Rat Expr. = $1.34654E - 05$ kg/s (Per 3 hours)

When the emission rates of the three roads and both expressways are completed, the results are taken as shown in Tables 21 and 22, which summarize the emission rates used in the simulations for the normal period and lockdown period, respectively. Then, the emission rate for each period is added in the Total Flow rate field as shown in Figure 11.

Table 21: A summary of the emission rates used in simulations during the normal period.

Emission rate (kg/s)	Periods		
	7 AM - 9 AM	10 AM – 12 PM	1 PM – 4 PM
Emission rate of Din Daeng rd.	5.53E-6	5.82E-6	8.74E-6
Emission rate of Pracha Songkhro rd.	1.16E-6	1.72E-6	2.58E-6
Emission rate of Mitmaitri rd.	1.09E-6	1.38E-6	2.08E-6
Emission rate of Chalerm Mahanakorn Expr.	1.18E-6	1.18E-6	1.77E-6
Emission rate of Si Rat Expr.	1.09E-5	1.09E-5	1.64E-5

Table 22: A summary of emission rates used in the simulations during the lockdown period.

Emission rate (kg/s)	Periods		
	7 AM - 9 AM	10 AM – 12 PM	1 PM – 4 PM
Emission rate of Din Daeng rd.	3.44E-6	4.75E-6	7.13E-6
Emission rate of Pracha Songkhro rd.	7.29E-7	1.40E-6	2.11E-6
Emission rate of Mitmaitri rd.	6.82E-6	1.13E-6	1.70E-6
Emission rate of Chalerm Mahanakorn Expr.	9.71E-7	9.71E-7	1.46E-6
Emission rate of Si Rat Expr.	8.98E-6	8.98E-6	1.35E-5

When setting up the injections is done. Next, it will be set up. The boundary conditions (Salim Mohamed Salim et al., 2011; Xiaoxia Wang et al., 2020) are defined as follows.

- Inlet

Velocity Inlet

Zone Name: inlet

Momentum Thermal Radiation Species DPM Multiphase Potential UDS

Velocity Specification Method: Magnitude, Normal to Boundary

Reference Frame: Absolute

Velocity Magnitude (m/s): 0.2 constant

Supersonic/Initial Gauge Pressure (pascal): 0 constant

Turbulence

Specification Method: Intensity and Hydraulic Diameter

Turbulent Intensity (%): 5

Hydraulic Diameter (m): 506.4001

OK Cancel Help

Figure 12: Setting inlet boundary conditions.

To define the inlet from Figure 12, the velocity specification method will be set to Magnitude, Normal to Boundary, or come out in the perpendicular direction. The wind direction to be used in the model was taken from the mean wind direction during the study period (P. C. Department, 2019-2021b; H.H. Niu et al., 2018). It is shown in Table 23. From 7 AM - 4 PM, the wind direction will come from the same direction as shown in Figure 13.

Table 23: Wind direction is used in both normal and lockdown periods.

Periods	Wind Directions (Deg.M)	
	Normal period	Lockdown period
7 AM – 9 AM	222 (←)	224.3 (←)
10 AM – 12 PM	195.3 (←)	213.3 (←)
1 PM – 4 PM	171 (←)	174.75 (←)

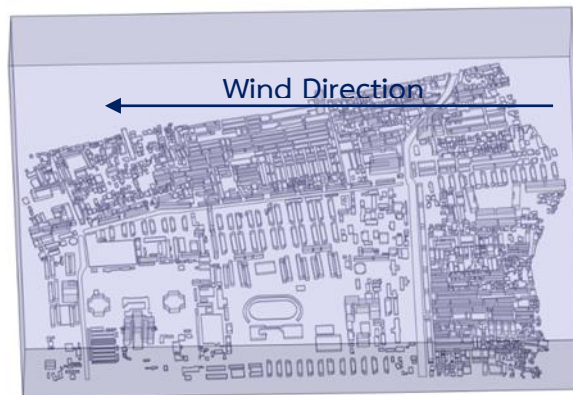


Figure 13: Wind direction from 7 AM – 4 PM

As shown in Table 24, the reference frame is defined as Absolute (Default), and Velocity Magnitude is defined as the mean wind speed during the study period.

Table 24: Mean wind speed is used in both normal and lockdown periods.

Periods	Wind Speeds (m/s)	
	Normal period	Lockdown period
7 AM – 9 AM	0.20	0.10
10 AM – 12 PM	0.43	0.20
1 PM – 4 PM	0.775	0.45

Turbulence uses intensity and hydraulic diameter as shown in Table 25.

Table 25: Turbulence Setup.

Turbulence	
Specification Method	Intensity and Hydraulic Diameter
Turbulent Intensity (%)	5 (Default)
Hydraulic Diameter (m)	Calculated from $DH = 2ab/a+b$

By calculating Hydraulic Diameter (m) from Equation (30) (Daniel(Jian) Sun & Zhang, 2018)

$$DH = 2ab/a+b \quad (30)$$

In the presence of expressways, the width (a) and height (b) are shown in Figure 14.

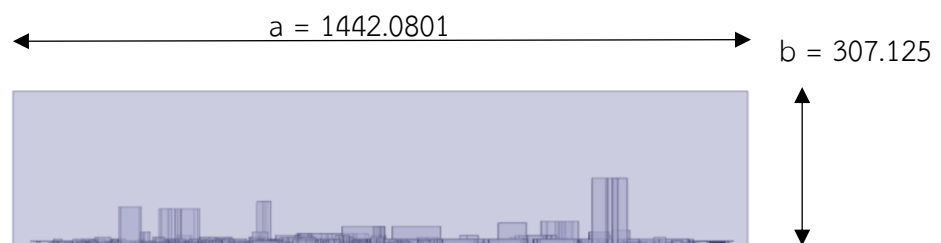


Figure 14: The width and height of the study area in the presence of expressways.

will result in a hydraulic diameter of 506.40

In the absence of expressways, it has width (a) and height (b) as shown in Figure 15.

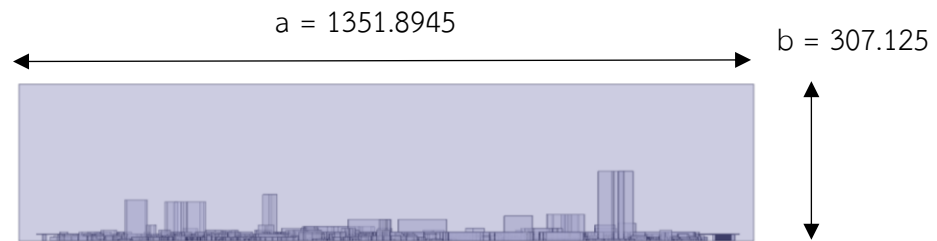


Figure 15: The width and height of the study area in the absence of expressways.

will result in a hydraulic diameter of 500.54

Table 26: Hydraulic Diameter in both cases with/without expressways.

Scenarios	Hydraulic Diameter
With Expressways	506.40
Without Expressways	500.54

K and Epsilon (Hong et al., 2017; Sun & Zhang, 2018) calculated from

Turbulent kinetic energy, k :

$$k = \frac{3}{2} (u_{avg} I)^2 \quad (31)$$

$$k = \frac{3}{2} [0.2(0.05)]^2 = 0.00015 \text{ m}^2/\text{s}^2$$

where u_{avg} is the mean flow velocity (m/s), I is the turbulence intensity, ρ is air density (kg/m^3), μ is viscosity of air (kg/ms), u is the air velocity (m/s) and D_H is hydraulic diameter

Turbulent Dissipation Rate, \mathcal{E} :

$$\mathcal{E} = \frac{k^{3/2}}{l} \quad (32)$$

where l is the turbulence length scale, C_μ is the constant = 0.09

$$l = \frac{0.07D_H}{C_\mu^{3/4}} \quad (33)$$

$$\varepsilon = \frac{k^{3/2}C_\mu^{3/4}}{0.07D_H} = \frac{(0.00015)^{3/2} \times 0.09^{3/4}}{0.07 \times 506.40}$$

$$\varepsilon = 8.51 \times 10^{-9} \text{ m}^2/\text{s}^3$$

Thermal designation as shown in Figure 16. Temperature is determined as the mean temperature during the study period as shown in Table 27.

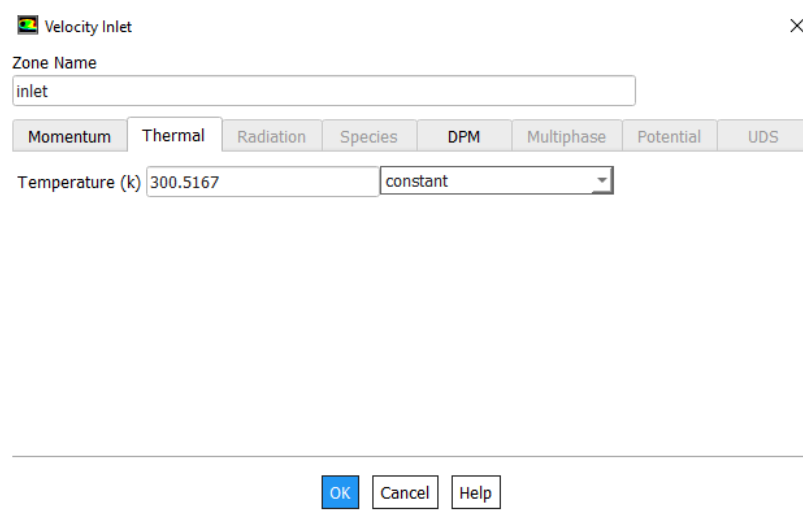


Figure 16: Inlet Temperature Setting.

Table 27: Mean temperatures are used in simulations for both normal and lockdown periods.

Periods	Temperature (K)	
	Normal period	Lockdown period
7 AM – 9 AM	300.52	299.75
10 AM – 12 PM	305.92	303.72
1 PM – 4 PM	306.43	305.70

The DPM in the inlet is set as an escape, as shown in Figure 17.

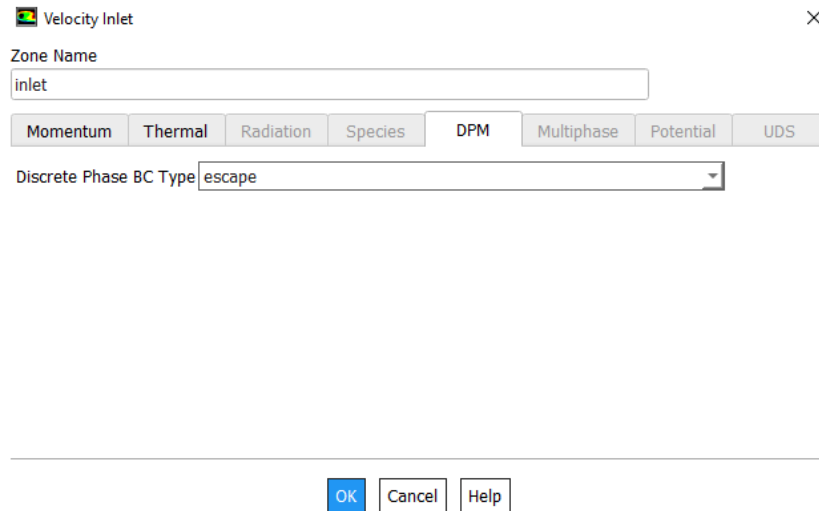


Figure 17: Inlet DPM Settings.

- Outlet

The outlet momentum are set as shown in Table 28.

Table 28: Outlet Momentum Settings.

Momentum	
Backflow Reference Frame	Absolute
Gauge Pressure (pascal)	0
Pressure Profile Multiplier	1
Backflow Direction Specification Method	Normal to Boundary
Backflow Pressure Specification	Total Pressure
Turbulence	
Specification Method	Intensity and Hydraulic Diameter
Backflow Turbulent Intensity (%)	5 (Default)
Backflow Hydraulic Diameter (m)	According to table 3.27

Thermal designation is defined as the mean temperature during the study period, as shown in Table 27, and the outlet DPM is defined as escape.

- Roads, Expressways, and Ground

The Momentum of roads, expressway, and ground are set as shown in Table 29.

Table 29: Roads, Expressways, and Ground Momentum Settings.

Momentum	
Wall Motion	Stationary Wall
Shear Condition	No Slip
Wall Roughness	
Roughness Model	Standard
Sand-Grain Roughness	
Roughness Height (m)	0 (Default)
Roughness Constant	0.5 (Default)

Thermal designation is defined as the mean temperature during the study period plus 13 as the road temperature. DPM on roads, expressways, and ground is defined as reflect, as shown in Table 30.

Table 30: Mean Road temperatures are used in both normal and lockdown periods.

Periods	Temperature (K)	
	Normal period	Lockdown period
7 AM – 9 AM	313.52	312.75
10 AM – 12 PM	318.92	316.72
1 PM – 4 PM	319.43	318.70

- Upper and lateral boundaries are defined as symmetry

Then set the solution used in the model. The Methods section is defined as shown in Table 31 and the Controls as shown in Table 32. After that, run calculation with the number of iterations of 2000.

Table 31: Method Settings.

Pressure-Velocity Coupling	
Scheme	SIMPLE
Spatial Discretization	
Gradient	Least Squares Cell Based
Pressure	Second Order
Momentum	Second Order Upwind
Turbulent Kinetic Energy	First Order Upwind
Turbulent Dissipation Rate	First Order Upwind
carbon	Second Order Upwind
Energy	Second Order Upwind

Table 32: Control Settings.

Under-Relaxation Factors	
Pressure	0.3
Density	1.0
Body Forces	1.0
Momentum	0.7
Turbulent Kinetic Energy	0.8
Turbulent Dissipation Rate	0.8
Turbulent Viscosity	1.0
carbon	1.0
Energy	1.0

Chapter 4

Results and Discussion

4.1 Model Validation

Model validation is the process of verifying a model by comparing it to experimental data. In this study, the data from the simulation is compared with the measured data from Bangkok's air quality monitoring station (b56). The measurements are made at a height of 2.5 meters above the ground (6, 2009), where the air quality monitoring equipment is installed. There will be two parts to the model validation, as shown below.

4.1.1 Discrete Phase Model Validation Results: January 27 2020 (Normal period).

Simulation results from 7 AM to 9 AM

- The concentration of $PM_{2.5}$ in the area near the air quality monitoring station.

Table 33: A comparison of $PM_{2.5}$ concentrations on January 27, 2020, from 7 AM - 9 AM.

$PM_{2.5}$ concentration obtained from the air quality monitoring station	$PM_{2.5}$ concentration obtained from simulation
52.33 micrograms per square meter	10,423.24 micrograms per square meter

- Temperature in the area near the air quality monitoring station.

Table 34: A comparison of temperatures on January 27, 2020, from 7 AM - 9 AM.

Temperature obtained from the air quality monitoring station	Temperature obtained from simulation
300.52 K	307.78 K

- Velocity in the area near the air quality monitoring station.

Table 35: A comparison of wind speeds on January 27, 2020, from 7 AM - 9 AM.

Velocity obtained from the air quality monitoring station	Velocity obtained from simulation
0.2 meter per sec	0.05 meter per sec

Simulation results from 10 AM to 12 PM

- The concentration of $PM_{2.5}$ in the area near the air quality monitoring station.

Table 36: A comparison of $PM_{2.5}$ concentrations on January 27, 2020, from 10 AM - 12 PM.

PM _{2.5} concentration obtained from the air quality monitoring station	PM _{2.5} concentration obtained from simulation
37.67 micrograms per square meter	8,729.89 micrograms per square meter

- Temperature in the area near the air quality monitoring station.

Table 37: A comparison of temperatures on January 27, 2020, from 10 AM - 12 PM.

Temperature obtained from the air quality monitoring station	Temperature obtained from simulation
305.92 K	309.99 K

- Velocity in the area near the air quality monitoring station.

Table 38: A comparison of wind speeds on January 27, 2020, from 10 AM - 12 PM.

Velocity obtained from the air quality monitoring station	Velocity obtained from simulation
0.43 meter per sec	0.2 meter per sec

4.1.2 Discrete Phase Model Validation Results: January 25 2021 (Lockdown period)

Simulation results from 7 AM to 9 AM

- The concentration of $PM_{2.5}$ in the area near the air quality monitoring station.

Table 39: A comparison of PM_{2.5} concentrations on January 25, 2021, from 7 AM – 9 AM.

PM _{2.5} concentration obtained from the air quality monitoring station	PM _{2.5} concentration obtained from simulation
21 micrograms per square meter	955.61 micrograms per square meter

- Temperature in the area near the air quality monitoring station.

Table 40: A comparison of temperatures on January 25, 2021, from 7 AM – 9 AM.

Temperature obtained from the air quality monitoring station	Temperature obtained from simulation
299.75 K	304.62K

- Velocity in the area near the air quality monitoring station.

Table 41: A comparison of wind speeds on January 25, 2021, from 7 AM – 9 AM.

Velocity obtained from the air quality monitoring station	Velocity obtained from simulation
0.1 meter per sec	0.02 meter per sec

Simulation results from 10 AM to 12 PM

- The concentration of PM_{2.5} in the area near the air quality monitoring station.

Table 42: A comparison of PM_{2.5} concentrations on January 25, 2021, from 10 AM – 12 PM.

PM _{2.5} concentration obtained from the air quality monitoring station	PM _{2.5} concentration obtained from simulation
24 micrograms per square meter	2,352 micrograms per square meter

- Temperature in the area near the air quality monitoring station.

Table 43: A comparison of temperatures on January 25, 2021, from 10 AM – 12 PM.

Temperature obtained from the air quality monitoring station	Temperature obtained from simulation
303.72 K	308.58 K

- Velocity in the area near the air quality monitoring station.

Table 44: A comparison of wind speeds on January 25, 2021, from 9 AM – 12 PM.

Velocity obtained from the air quality monitoring station	Velocity obtained from simulation
0.2 meter per sec	0.05 meter per sec

Simulation results from 1 PM to 4 PM

- The concentration of PM_{2.5} in the area near the air quality monitoring station.

Table 45: A comparison of PM_{2.5} concentrations on January 25, 2021, from 1 PM – 4 PM.

PM _{2.5} concentration obtained from the air quality monitoring station	PM _{2.5} concentration obtained from simulation
30.5 micrograms per square meter	5862.61 micrograms per square meter

- Temperature in the area near the air quality monitoring station.

Table 46: A comparison of temperatures on January 25, 2021, from 1 PM – 4 PM.

Temperature obtained from the air quality monitoring station	Temperature obtained from simulation
305.7 K	310.44 K

- Velocity in the area near the air quality monitoring station.

Table 47: A comparison of wind speeds on January 25, 2021, from 1 PM – 4 PM.

Velocity obtained from the air quality monitoring station	Velocity obtained from simulation
0.45 meter per sec	0.11 meter per sec

Comparison of the measured values from the air quality monitoring station with the simulation results.

Table 48: PM_{2.5} concentrations at the air quality monitoring station were compared to the results obtained from the three time periods on January 27, 2020.

Time	PM _{2.5} Concentration ($\mu\text{g}/\text{m}^3$)	
	Measurement	Simulation
7 AM – 9 AM	52.33	10,423.24
10 AM – 12 PM	37.67	8,729.89

Table 49: PM_{2.5} concentrations at the air quality monitoring station were compared to the results obtained from the three time periods on January 25, 2021.

Time	PM _{2.5} Concentration ($\mu\text{g}/\text{m}^3$)	
	Measurement	Simulation
7 AM – 9 AM	21	955.61
10 AM – 12 PM	24	2,352
1 PM – 4 PM	30.5	5862.61

The $PM_{2.5}$ concentrations from the air quality monitoring station and the simulation results for normal and lockdown periods are compared in Tables 48 and 49. It is evident that the simulation's results are greater than the measurements from the air quality monitoring station. Therefore, it is necessary to identify a correction factor to ensure that the value obtained from the simulation is comparable to the value acquired from the air quality monitoring station. This correction factor will be identified from the correlation of the data as shown in Figure 18.

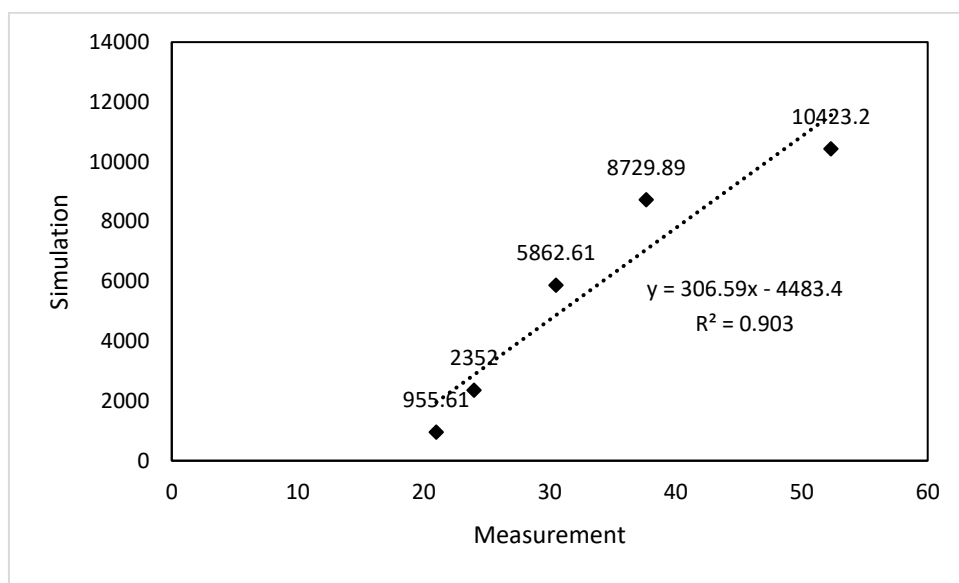


Figure 18: Relationship between $PM_{2.5}$ concentrations from measurement data and simulation results.

From Figure 18, the relationship between the simulation results and the values obtained from the air quality monitoring station is equal to Simulation results = $306.59(\text{Measurement data}) - 4483.4$, therefore the correction factor is 0.00326.

Table 50: Multiply the correction factor by 0.00326 so that the simulation results are close to the values obtained at the air quality monitoring station on January 27, 2020.

Time	PM _{2.5} Concentration ($\mu\text{g}/\text{m}^3$)	
	Measurement	Simulation
7 AM – 9 AM	52.33	33.98
10 AM – 12 PM	37.67	28.46

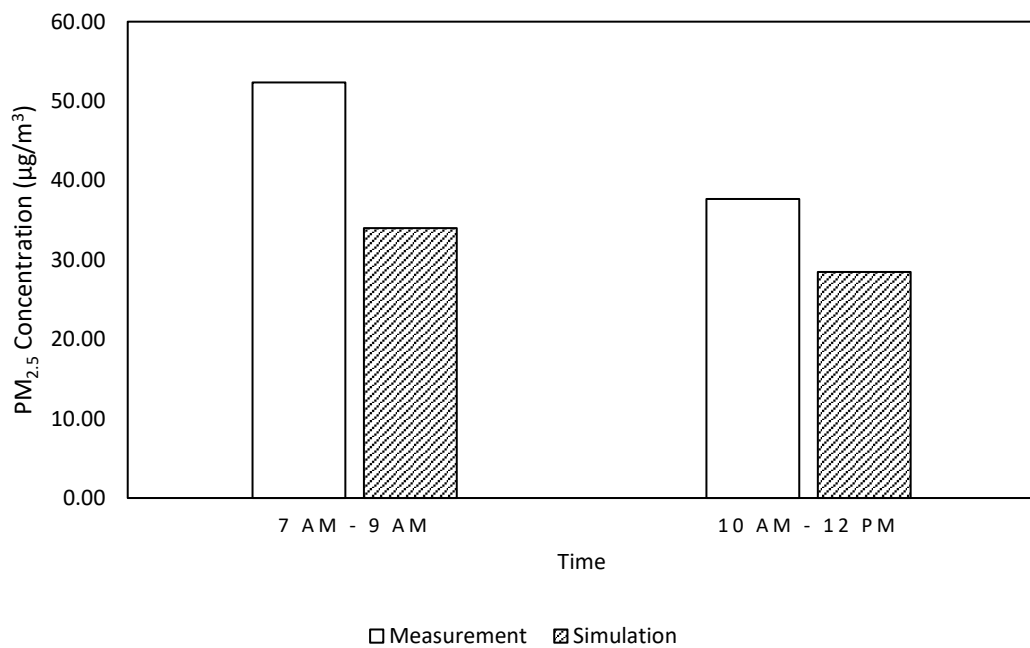


Figure 19: A comparison between the PM_{2.5} concentrations measured at the air quality monitoring station and the simulation results on January 27, 2020.

From Figure 19, the trend of PM_{2.5} concentrations obtained from the air quality monitoring station tends to decrease. This corresponds to the values obtained from the simulations that are also trending downward.

Table 51: Temperatures at the air quality monitoring station were compared with the simulation results obtained from the three time periods on January 27, 2020.

Time	Temperature (K)	
	Measurement	Simulation
7 AM – 9 AM	300.52	307.78
10 AM – 12 PM	305.92	309.99

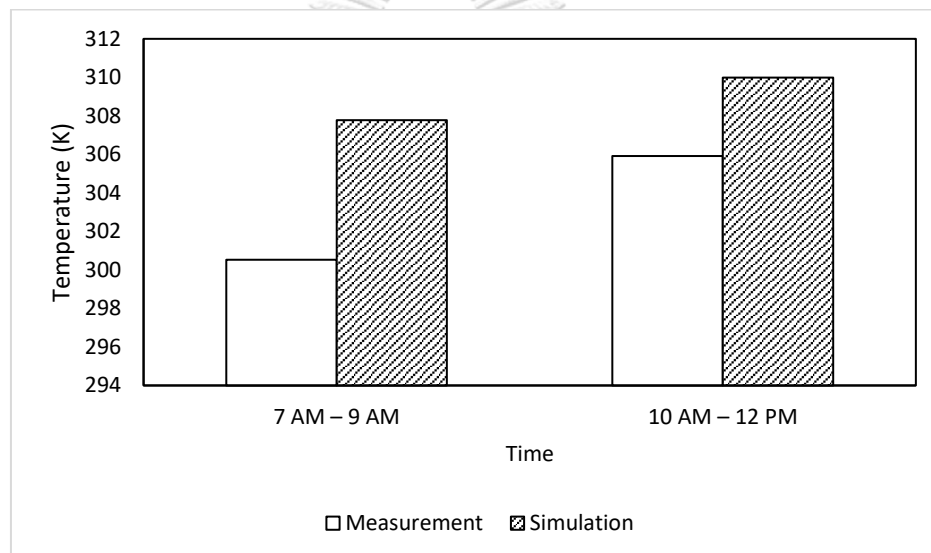


Figure 20: A comparison between the temperatures measured at the air quality monitoring station and the simulation results on January 27, 2020.

Table 52: Velocities at the air quality monitoring station were compared with the simulation results obtained from the three time periods on January 27, 2020.

Time	Velocity (m/s)	
	Measurement	Simulation
7 AM – 9 AM	0.2	0.05
10 AM – 12 PM	0.43	0.2

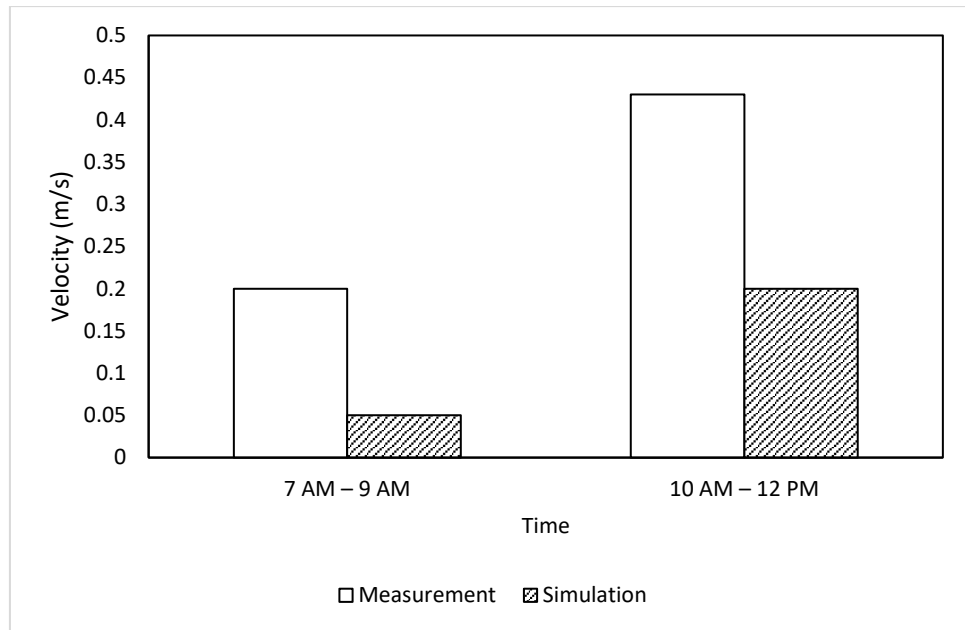


Figure 21: A comparison between the velocities measured at the air quality monitoring station and the simulation results on January 27, 2020.

Comparison of the measured values from the air quality monitoring station with the simulation results obtained from the lockdown periods.

Table 53: Multiply the correction factor by 0.00326 so that the simulation results are close to the values obtained at the air quality monitoring station on January 25, 2021

Time	PM _{2.5} Concentration ($\mu\text{g}/\text{m}^3$)	
	Measurement	Simulation
7 AM - 9 AM	21	3.12
10 AM - 12 PM	24	7.67
1 PM - 4 PM	30.5	19.11

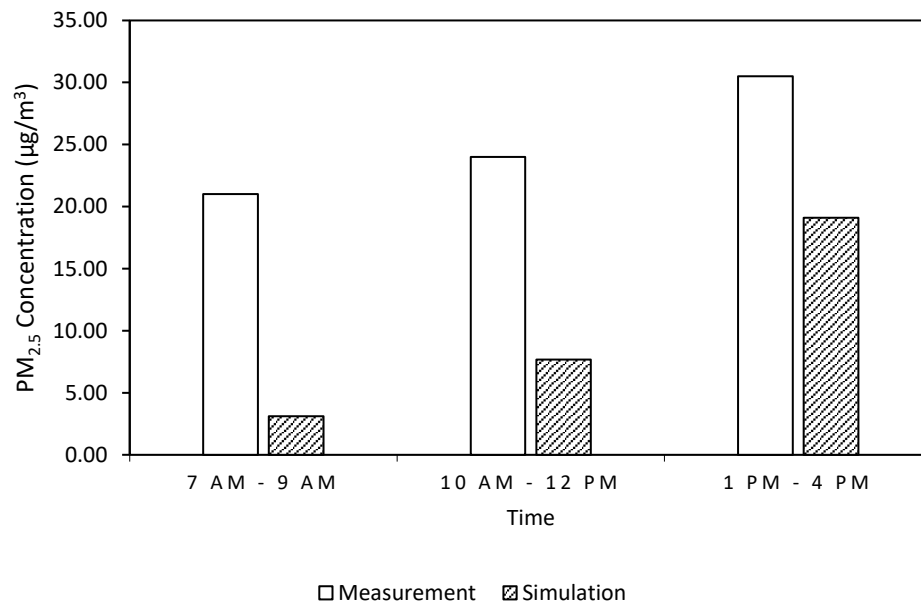


Figure 22: A comparison between the PM_{2.5} concentrations measured at the air quality monitoring station and the simulation results on January 25, 2021.

From Figure 22, the trend of PM_{2.5} concentration obtained from the air quality monitoring station tends to increase. This corresponds to the values obtained from the simulations that tend to increase as well.

Table 54: Temperatures at the air quality monitoring station were compared with the simulation results obtained from the three time periods on January 25, 2021.

Time	Temperature (K)	
	Measurement	Simulation
7 AM – 9 AM	299.75	304.62
10 AM – 12 PM	303.72	308.58
1 PM – 4 PM	305.7	310.44

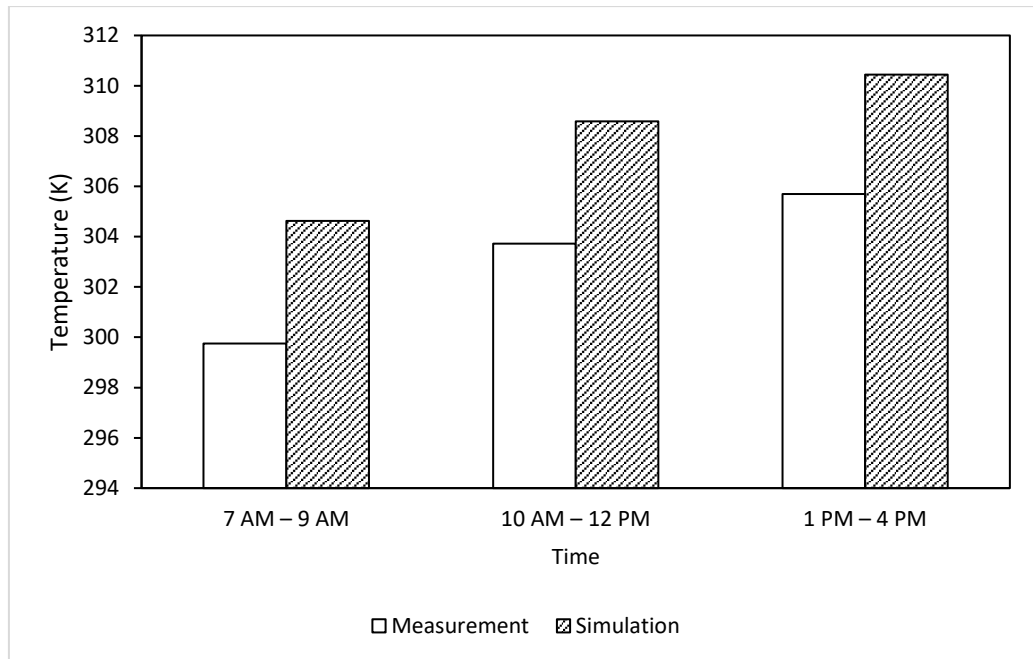


Figure 23: A comparison between the temperatures measured at the air quality monitoring station and the simulation results on January 25, 2021.

Table 55: Velocities at the air quality monitoring station were compared with the simulation results obtained from the three time periods on January 25, 2021.

Time	Velocity (m/s)	
	Measurement	Simulation
7 AM - 9 AM	0.1	0.02
10 AM - 12 PM	0.2	0.05
1 PM - 4 PM	0.45	0.11

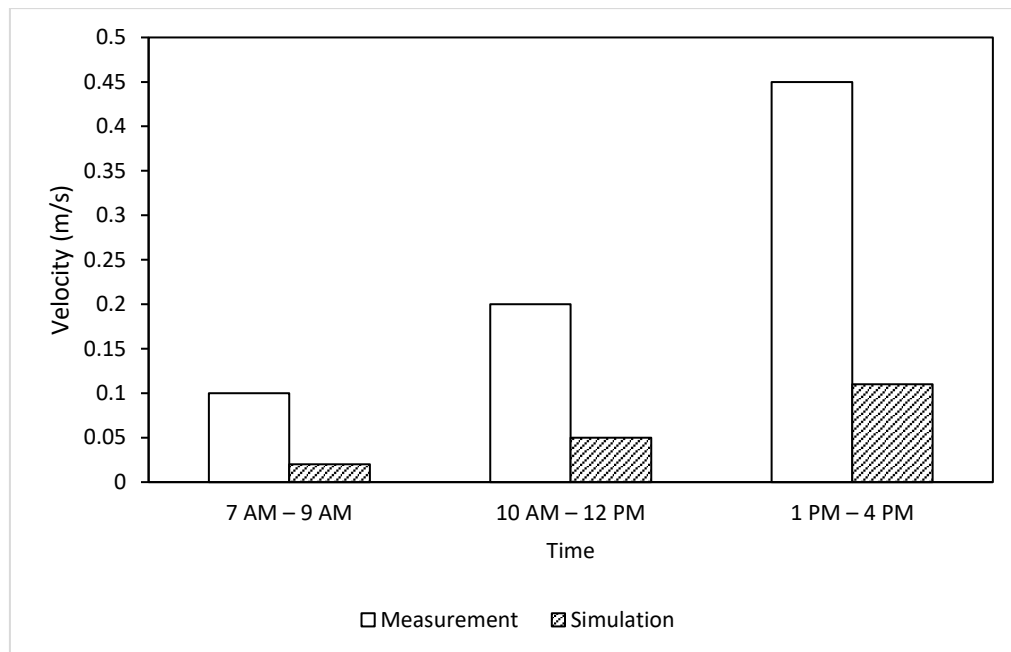


Figure 24: A comparison between the velocities measured at the air quality monitoring station and the simulation results on January 25, 2021.

From the model validation, it was found that the results of the simulations were consistent with the results obtained from the air quality monitoring station, so this numerical model could be used to study the dispersion of $PM_{2.5}$.

4.2 The influence of the expressways

The expressway structure in Din Daeng will consist of two expressways: the Si Rat Expressway, and the Chalem Mahanakhon Expressway. The presence of the expressways will increase the amount of traffic passing through that area, leading to the accumulation of more pollution in the area. Therefore, in this study, the existence of the expressways has been studied and how it affects the concentration of $PM_{2.5}$, which has the following results:

Simulation results from 7 AM to 9 AM

- The concentration of $PM_{2.5}$ in the area near the air quality monitoring station.

Table 56: A comparison of $PM_{2.5}$ concentrations on January 27, 2020, from 7 AM – 9 AM when there are no expressways.

$PM_{2.5}$ concentration obtained from the air quality monitoring station	$PM_{2.5}$ concentration obtained from simulation
52.33 micrograms per square meter	2,983.46 micrograms per square meter

- Temperature in the area near the air quality monitoring station.

Table 57: A comparison of temperatures on January 27, 2020, from 7 AM – 9 AM when there are no expressways.

Temperature obtained from the air quality monitoring station	Temperature obtained from simulation
300.52 K	304.92 K

- Velocity in the area near the air quality monitoring station.

Table 58: A comparison of wind speeds on January 27, 2020, from 7 AM – 9 AM when there are no expressways.

Velocity obtained from the air quality monitoring station	Velocity obtained from simulation
0.2 meter per sec	0.01 meter per sec

Simulation results from 10 AM to 12 PM

- The concentration of PM_{2.5} in the area near the air quality monitoring station.

Table 59: A comparison of PM_{2.5} concentrations on January 27, 2020, from 10 AM – 12 PM when there are no expressways

PM _{2.5} concentration obtained from the air quality monitoring station	PM _{2.5} concentration obtained from simulation
37.67 micrograms per square meter	2595.69 micrograms per square meter

- Temperature in the area near the air quality monitoring station.

Table 60: A comparison of temperatures on January 27, 2020, from 10 AM – 12 PM when there are no expressways

Temperature obtained from the air quality monitoring station	Temperature obtained from simulation
305.92 K	310.24 K

- Velocity in the area near the air quality monitoring station.

Table 61: A comparison of wind speeds on January 27, 2020, from 10 AM – 12 PM when there are no expressways

Velocity obtained from the air quality monitoring station	Velocity obtained from simulation
0.43 meter per sec	0.02 meter per sec

Comparison between the measured values from the air quality monitoring station with the simulation results without expressways.

Table 62: PM_{2.5} concentrations at the air quality monitoring station were compared to the results without expressways obtained from three time periods on January 27, 2020.

Time	PM _{2.5} Concentration ($\mu\text{g}/\text{m}^3$)	
	Measurement	Simulation
7 AM – 9 AM	52.33	2,983.46
10 AM – 12 PM	37.67	2,595.69

Table 63: Multiply the correction factor by 0.00326 so that the simulation results without expressways are close to the values obtained at the air quality monitoring station on January 27, 2020.

Time	PM _{2.5} Concentration ($\mu\text{g}/\text{m}^3$)	
	Measurement	Simulation
7 AM – 9 AM	52.33	9.73
10 AM – 12 PM	37.67	8.46

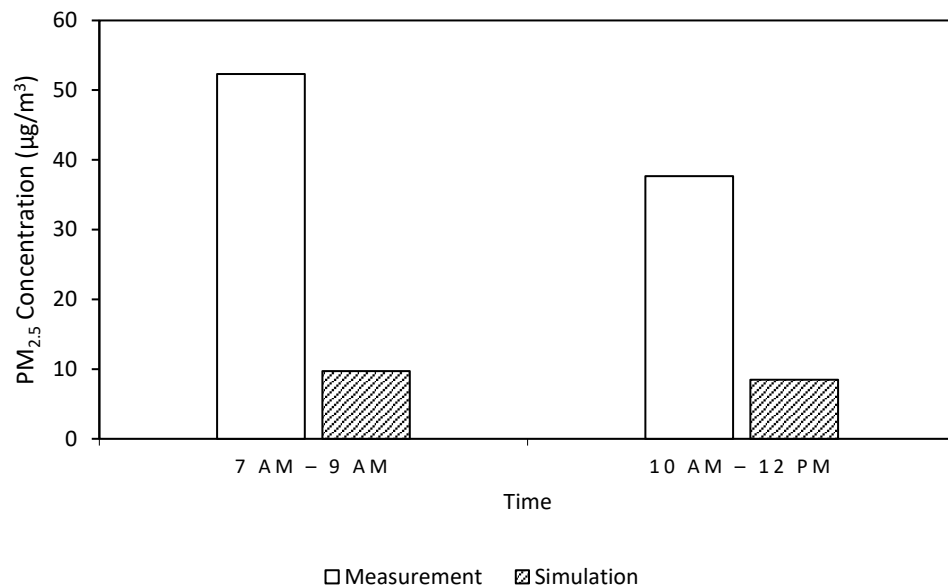


Figure 25: A comparison between the PM_{2.5} concentrations measured at the air quality monitoring station and the simulation results without expressways on January 27, 2020.

Figure 25 shows a comparison between the PM_{2.5} concentrations measured at the air quality monitoring station and the values obtained from the simulation results. In the absence of expressways, the PM_{2.5} concentration obtained from the measurement tends to decrease, like the air quality monitoring station. This corresponds to the values obtained from the simulations that are also trending downward.

Table 64: Temperatures at the air quality monitoring station were compared with the simulation results without expressways obtained from the three time periods on January 27, 2020.

Time	Temperature (K)	
	Measurement	Simulation
7 AM - 9 AM	300.52	304.92
10 AM - 12 PM	305.92	310.24

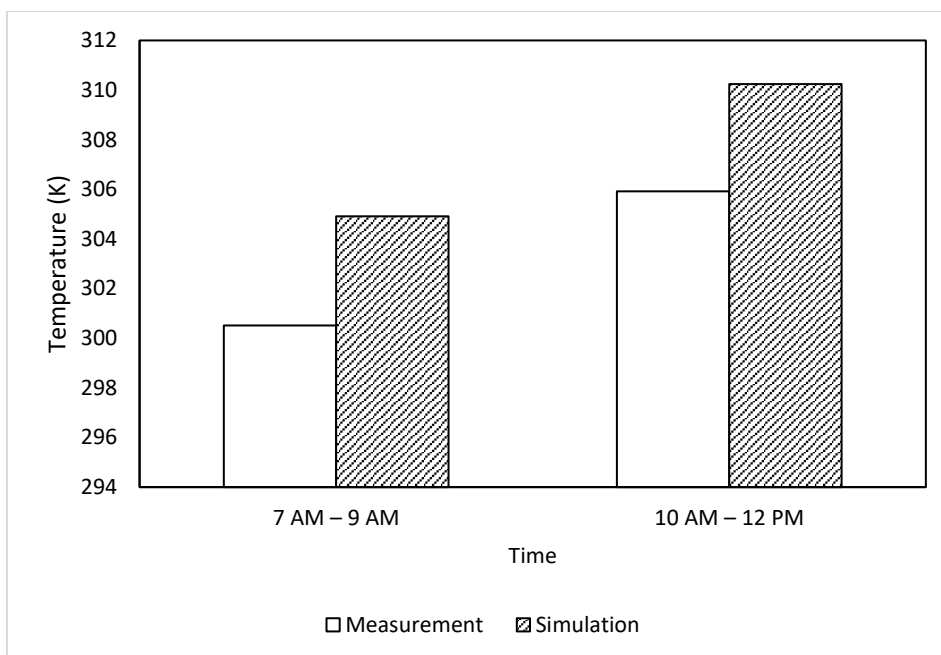


Figure 26: A comparison between the temperatures measured at the air quality monitoring station and the simulation results without expressways on January 27, 2020.

Table 65: Velocities at the air quality monitoring station were compared with the simulation results without expressways obtained from the three time periods on January 27, 2020.

Time	Velocity (m/s)	
	Measurement	Simulation
7 AM - 9 AM	0.2	0.01
10 AM - 12 PM	0.43	0.02

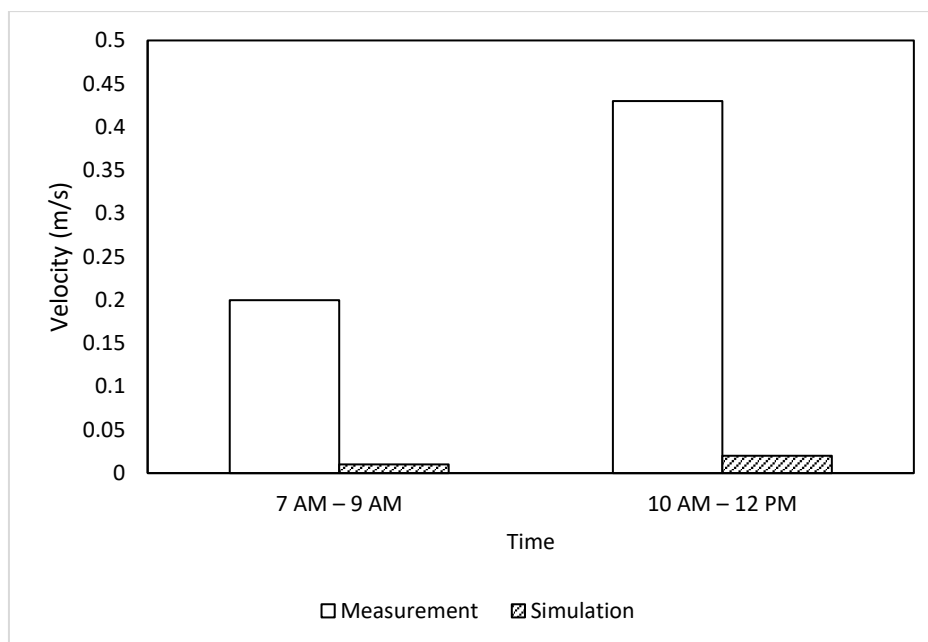


Figure 27: A comparison between the velocities measured at the air quality monitoring station and the simulation results without expressways on January 27, 2020.

Comparison of PM_{2.5} concentration, temperature, and wind speed obtained from measurements and simulations with and without expressways

Table 66: PM_{2.5} concentrations at the air quality monitoring station compared to the simulation results obtained from the three time periods. The results obtained from simulation multiply correction factor equal to 0.00326 to make the value close to the measured value from the air quality monitoring station.

Time	PM _{2.5} Concentration ($\mu\text{g}/\text{m}^3$)		
	Measurement	With Express	Without Express
7 AM - 9 AM	52.33	33.98	9.73
10 AM - 12 PM	37.67	28.46	8.46

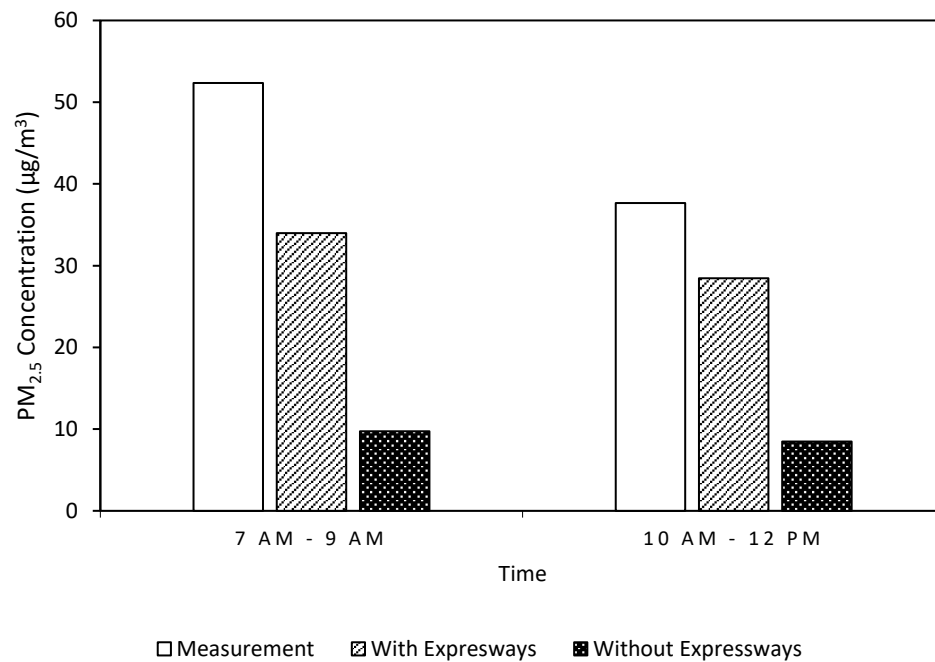


Figure 28: A comparison between PM_{2.5} concentrations measured at the air quality monitoring station and the values obtained from the simulation results in both cases.

Figure 28 shows a comparison between the PM_{2.5} concentration measured at the air quality monitoring station and the value obtained from the simulation results in both cases. In all cases, the PM_{2.5} concentration obtained from the air quality monitoring station, the values obtained from the simulation in the case of expressways, and the values obtained from the simulations without the expressways tend to decrease the PM_{2.5} concentration. By comparing the case with and without expressways, it was found that the presence of the expressway increased the concentration of PM_{2.5} by approximately 3.4 times compared to the case without expressways.

Table 67: Temperatures at the air quality monitoring station were compared to the simulation results obtained from the three time periods.

Time	Temperature (K)		
	Measurement	With Expressways	Without Expressways
7 AM – 9 AM	300.52	307.78	304.92
10 AM – 12 PM	305.92	309.99	310.24

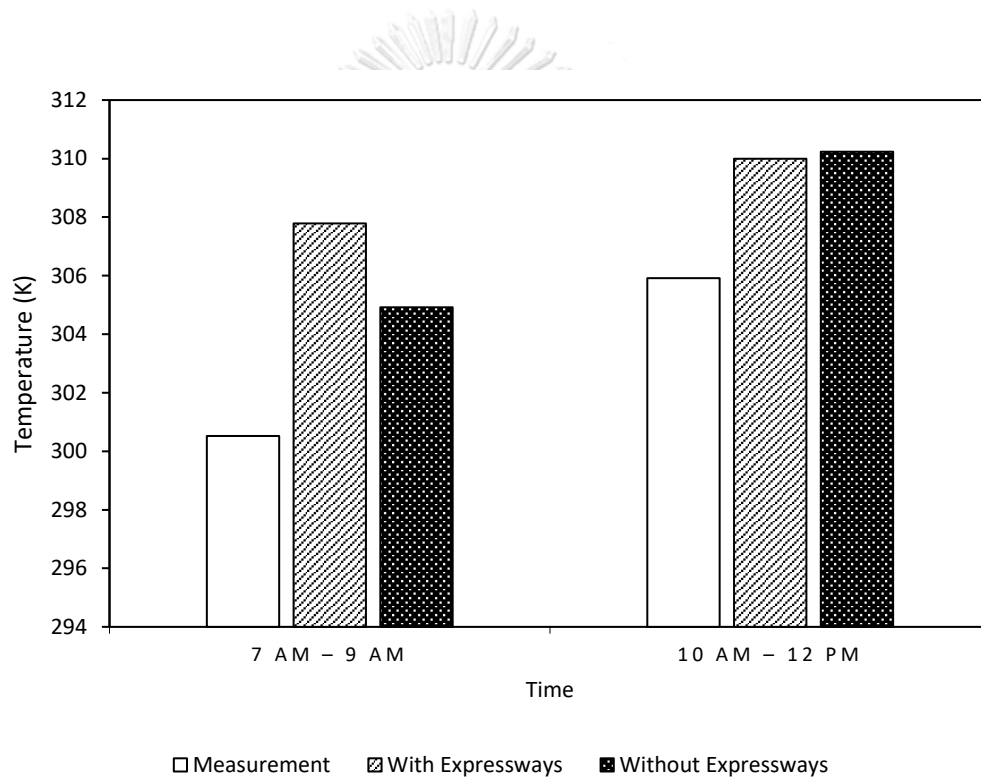


Figure 29: A comparison between temperatures measured at the air quality monitoring station and the values obtained from the simulation results in both cases.

Table 68: Velocities at the air quality monitoring station were compared to the simulation results obtained from the three time periods.

Time	Velocity (m/s)		
	Measurement	With Expressways	Without Expressways
7 AM – 9 AM	0.2	0.05	0.01
10 AM – 12 PM	0.43	0.2	0.02

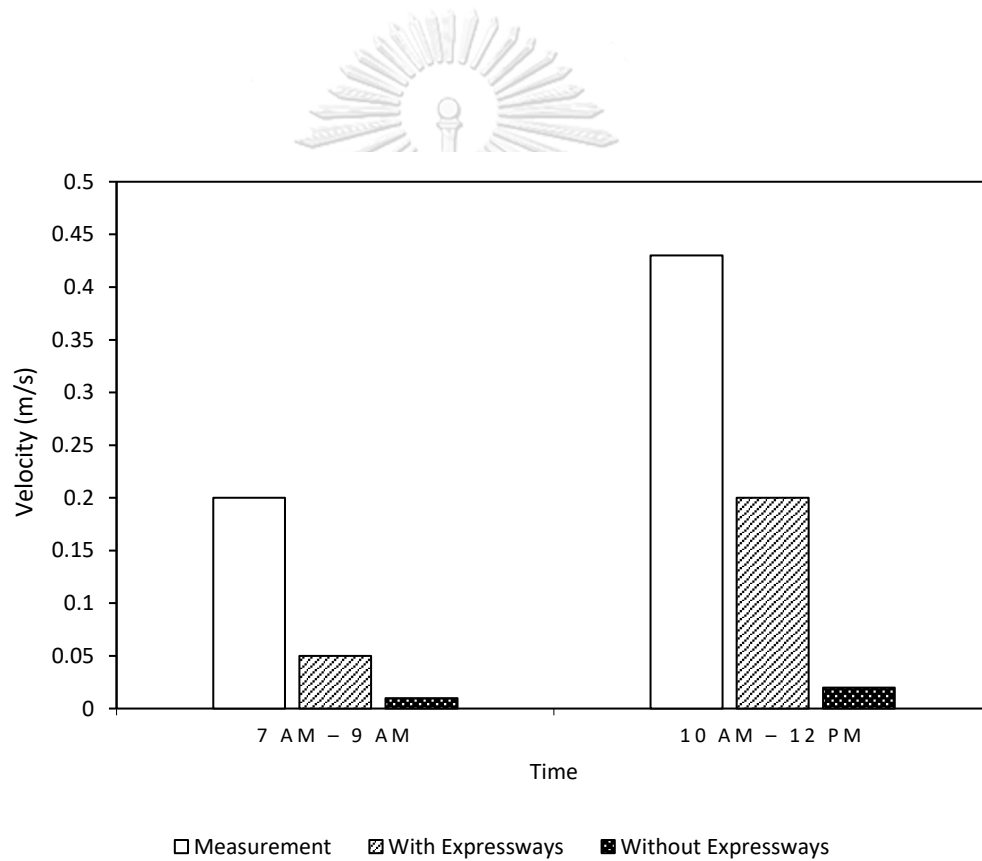


Figure 30: A comparison between velocities measured at the air quality monitoring station and the values obtained from the simulation results in both cases.

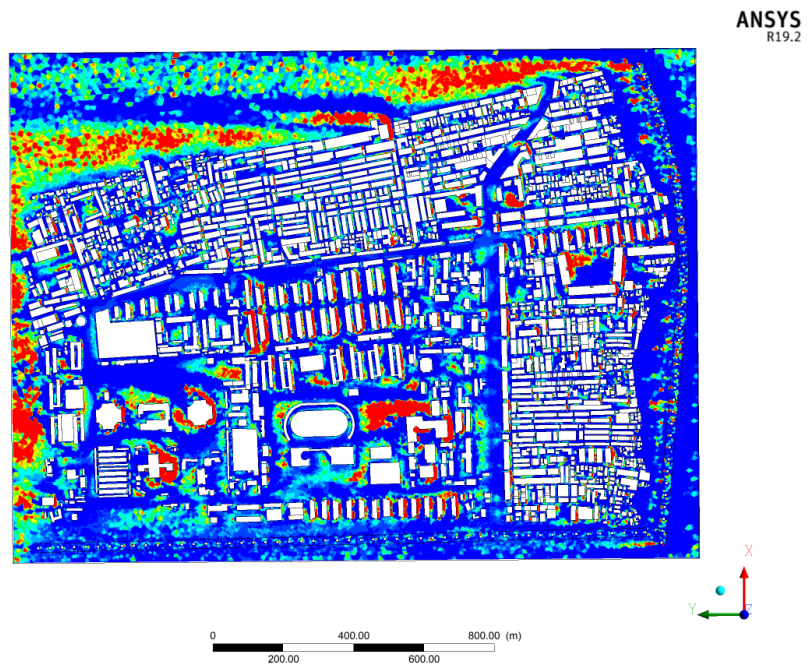


Figure 31: PM_{2.5} concentrations in the whole numerical model at 7 AM – 9 AM in the case of expressways.

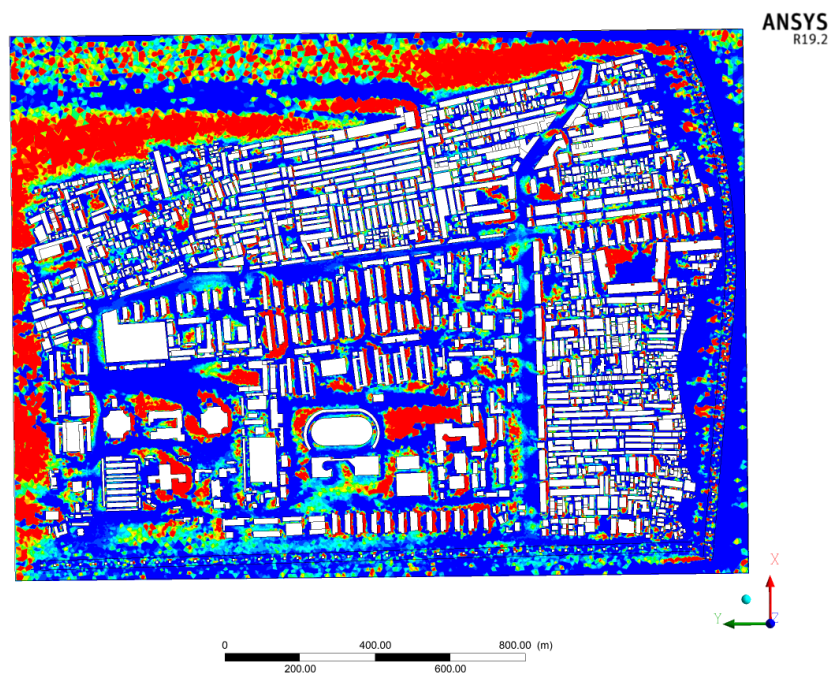


Figure 32: PM_{2.5} concentrations in the whole numerical model at 10 AM – 12 PM in the case of expressways.

From Figures 31 to 32, the concentration of $PM_{2.5}$ was discovered that the increase in emission rate through the numerical model shown in Table 75 will result in an increased $PM_{2.5}$ concentration. The highest $PM_{2.5}$ concentration is between 10 AM – 12 PM, which is the period with the highest emission rate, followed by 7 AM – 9 AM. The wind direction for the two periods will come from the right side.

Table 69: Wind speed, wind direction, and emission rate in each period.

	Periods	
	7 AM – 9 AM	10 AM – 12 PM
Wind speed (m/s)	0.2	0.43
Wind direction	←	←
Emission rate of Din Daeng rd. (kg/s)	5.53E-06	5.82E-06
Emission rate of Pracha Songkhro rd. (kg/s)	1.16E-06	1.72E-06
Emission rate of Mitmaitri rd. (kg/s)	1.09E-06	1.38E-06
Emission rate of Chalem Mahanakorn Expr. (kg/s)	1.18E-06	1.18E-06
Emission rate of Si Rat Expr. (kg/s)	1.09E-05	1.09E-05

Note: The emission rates of the Chalem Mahanakorn and the Si Rat Expressways are calculated from the monthly traffic volume.

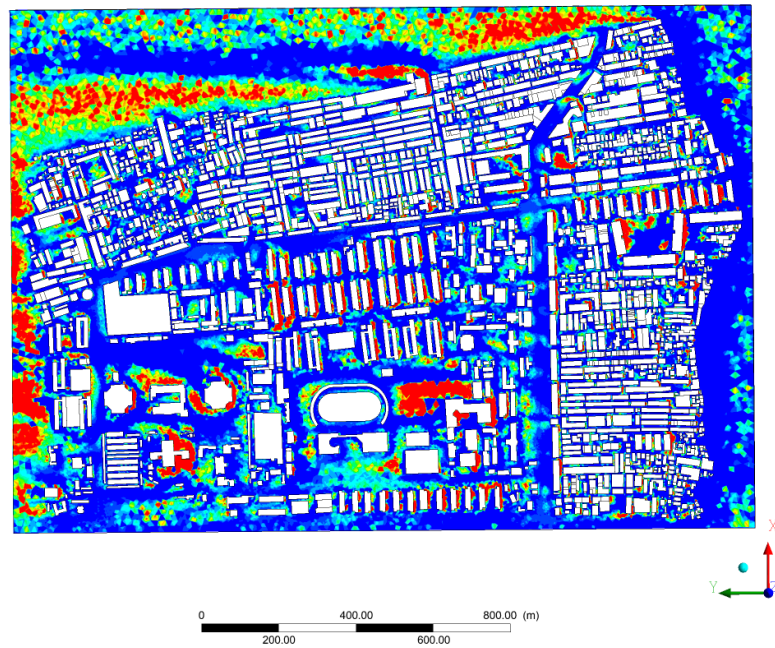


Figure 33: $PM_{2.5}$ concentrations in the whole numerical model at 7 AM – 9 AM in the case of no expressways.

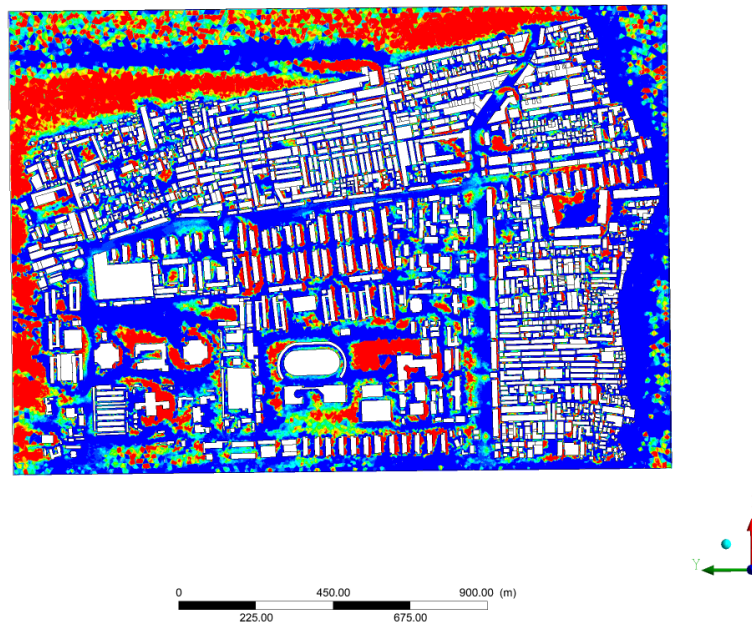


Figure 34: $PM_{2.5}$ concentrations in the whole numerical model at 10 AM – 12 PM in the case of no expressways.

PM_{2.5} concentration in the buildings near the expressway

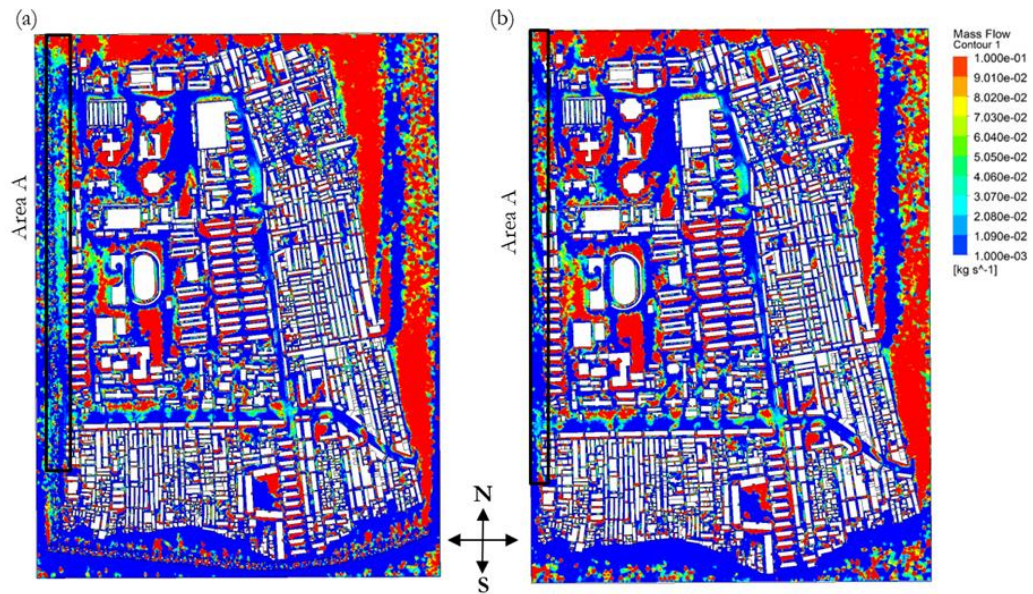


Figure 35: Mass flow of PM_{2.5} in Din Daeng district (simulated from traffic volume and meteorological data as of 27 January 2020 at 1-4 PM): (a) with expressways, (b) without expressways.

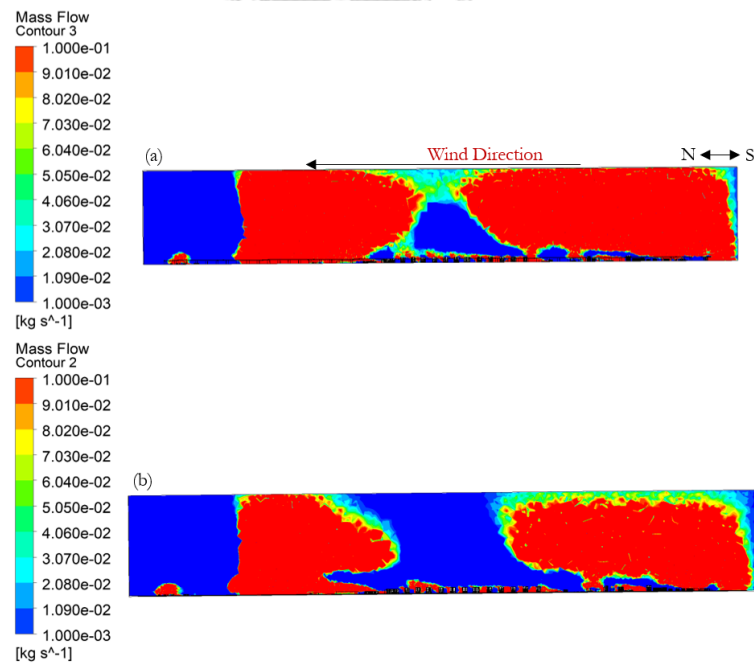


Figure 36: A cross-sectional plane of Mass flow of PM_{2.5} in area A (simulated from traffic volume and meteorological data as of 27 January 2020 at 1-4 PM): (a) with expressways, (b) without expressways.

Table 70: Emission rate and simulated meteorological results for the area near the expressway on Jan 27, 2020.

Time	Wind speed (m/s)	Wind direction	Temperature (K)	Emission rate (kg/s)
7 AM – 9 AM	0.05	←	307.78	5.53E-06
10 AM – 12 PM	0.2	←	309.99	5.82E-06
1 PM – 4 PM	0.36	←	316.33	8.74E-06

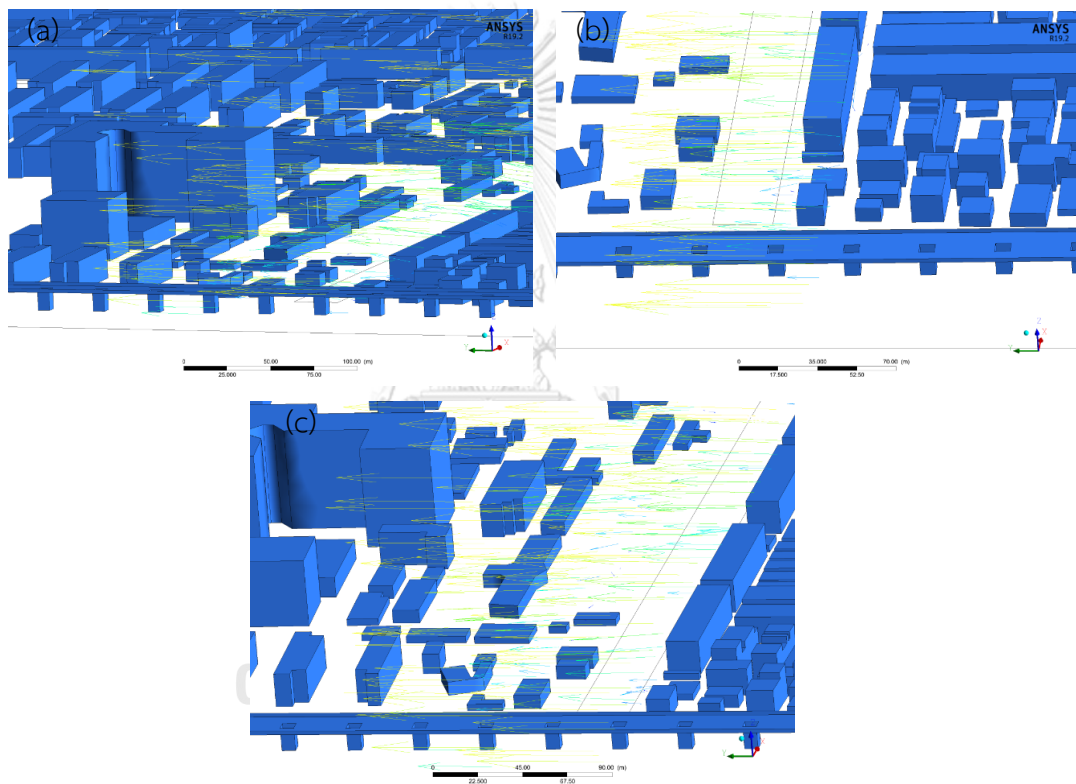


Figure 37: Airflow fields at the area near the expressway on Din Daeng Road during (a) 7-9 AM, (b) 10 AM – 12 PM, (c) 1-4 PM.

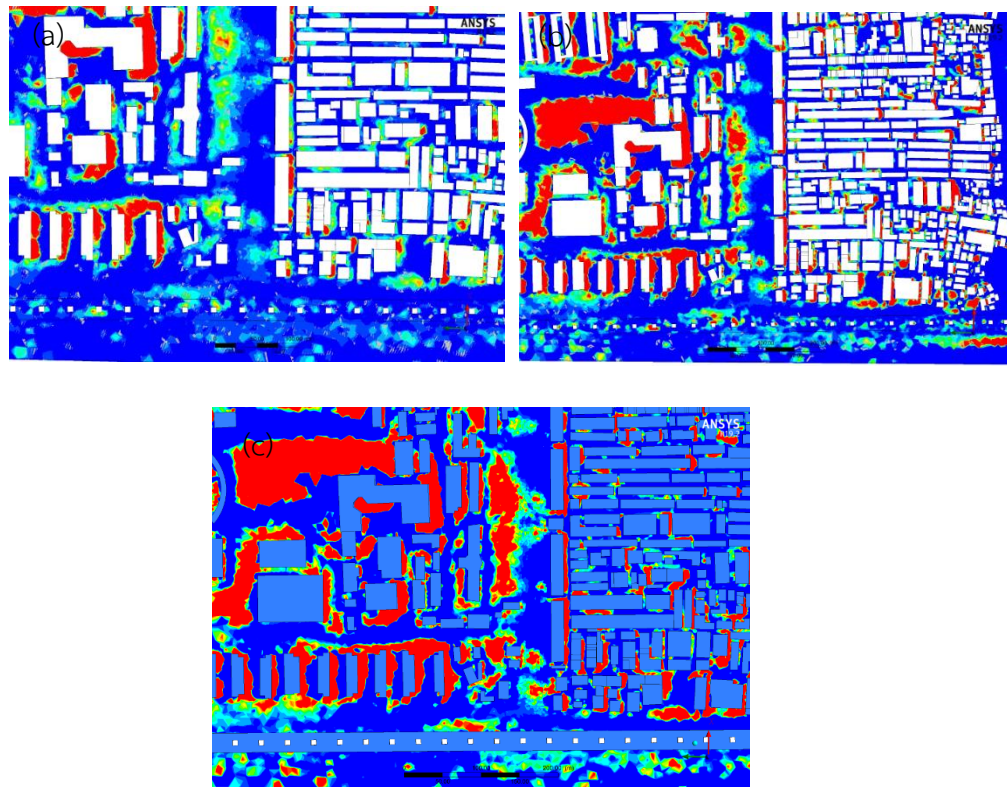


Figure 38: $PM_{2.5}$ concentration contour at the area near the expressway on Din Daeng Road during (a) 7-9 AM, (b) 10 AM – 12 PM, (c) 1-4 PM.

The influence of the expressways on the nearby buildings is shown in Figure 35, which shows the comparison of $PM_{2.5}$ mass flow in Din Daeng district in the presence and absence of the expressways at a height of 1.5 meters. It was discovered that the $PM_{2.5}$ concentration produced from the simulation with expressways was often greater than the $PM_{2.5}$ concentration in the simulation without expressways for the building close to the expressway at area A. Because it is surrounded by buildings and expressways, causing dust accumulation in that area. When comparing over time, it was found that the emission rate at Din Daeng Road increased over time, as shown in Table 70, resulting in an increase in $PM_{2.5}$ concentration over time as well, as shown in Figure 38.

PM_{2.5} concentration in high-rise building

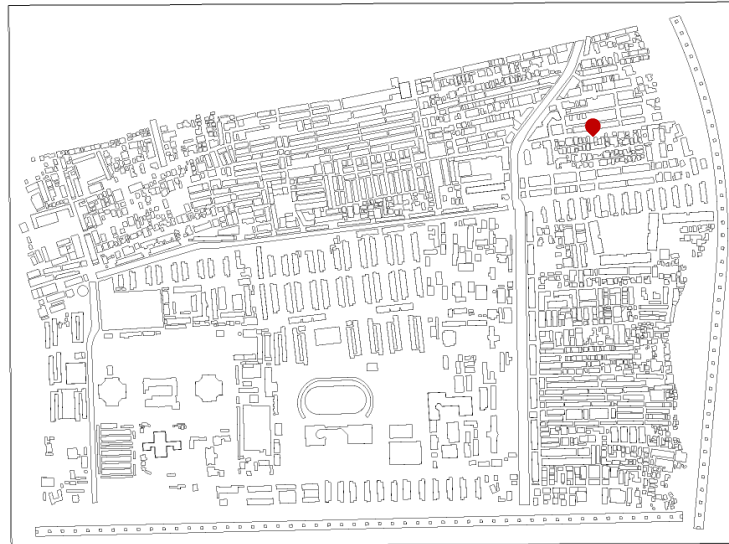


Figure 39: Location of PM_{2.5} concentration measurement points at high-rise buildings.

- The concentration of PM_{2.5}, obtained from the simulation in both cases

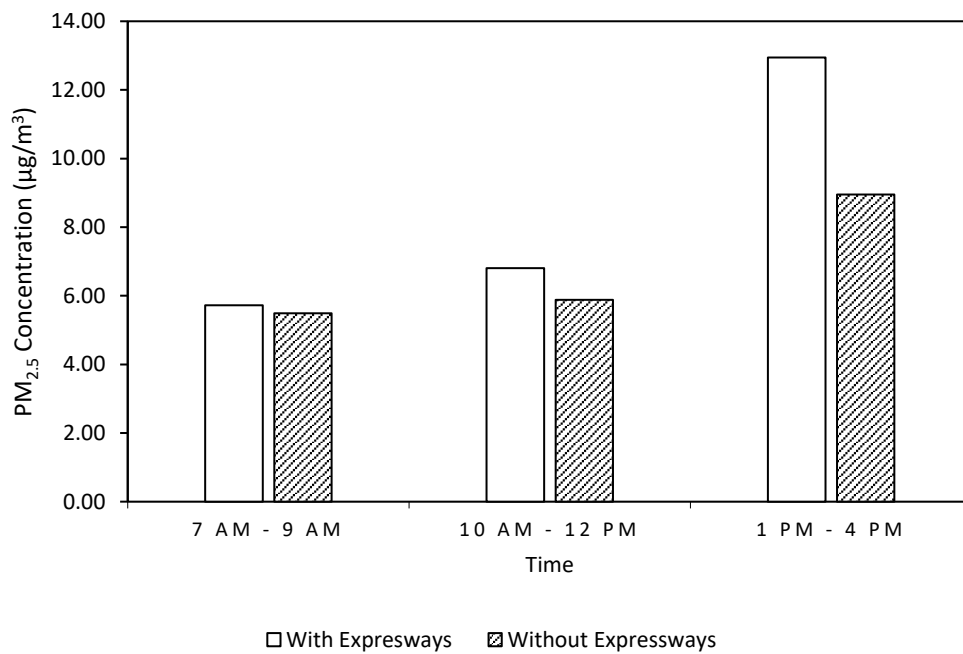


Figure 40: A comparison of PM_{2.5} concentrations in both simulations at the measurement point of the high-rise building.

When the wind comes from right to left, tall buildings block the direction of the wind. The $PM_{2.5}$ concentration in that area is not spread as shown in Figure 41. At 1 PM – 4 PM, the highest $PM_{2.5}$ concentration occurred because at that time the emission rate of Din Daeng Road, as shown in Table 70, was high.

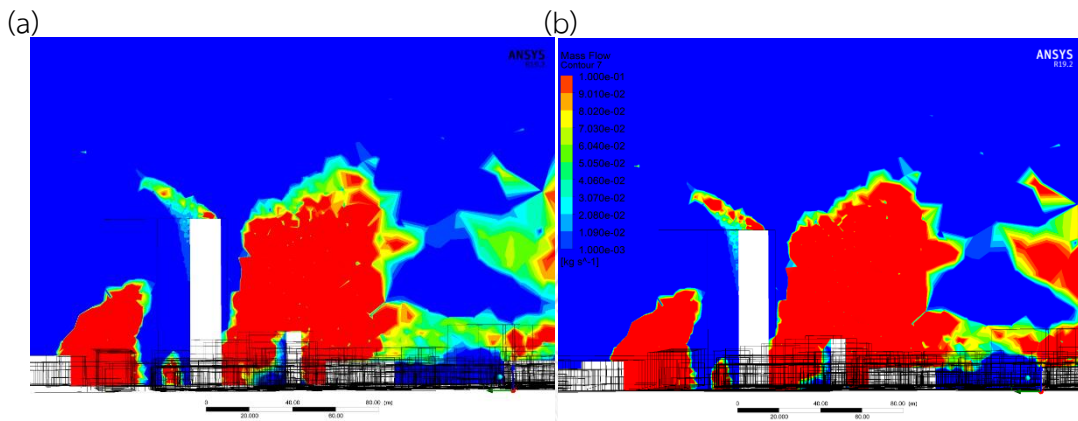


Figure 41: $PM_{2.5}$ dispersion on a cross-sectional plane at the high building during: (a) 10 AM – 12 PM, (b) 1 PM - 4 PM.

Table 71: A comparative result of $PM_{2.5}$ concentrations of both simulations at the measurement point of the high-rise building.

Time	$PM_{2.5}$ Concentration ($\mu\text{g}/\text{m}^3$)	
	With Expressways	Without Expressways
7 AM – 9 AM	5.73	5.49
10 AM – 12 PM	6.81	5.88
1 PM – 4 PM	12.95	8.95

Note: The $PM_{2.5}$ concentrations shown are multiplied by the correction factor equal to 0.00326.

PM_{2.5} concentration at various distances from the road

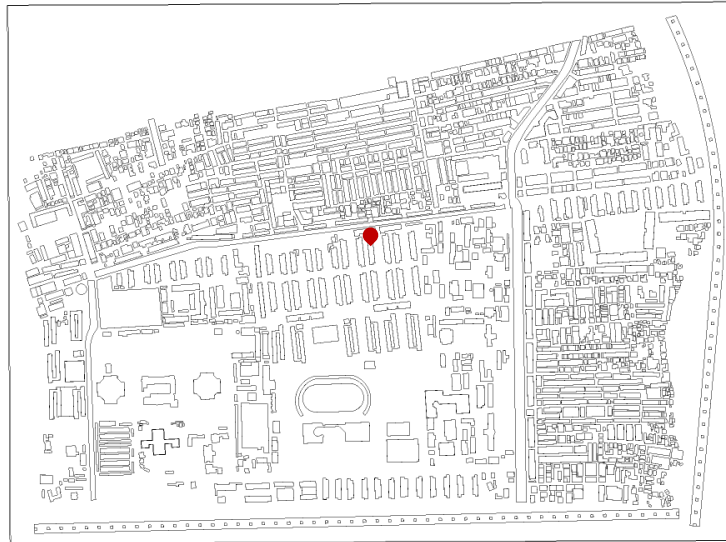


Figure 42: Location of concentration measurement points at different distances from the road.

- The concentration of PM_{2.5}, obtained from the simulation in both cases, ranges from 1 PM – 4 PM.

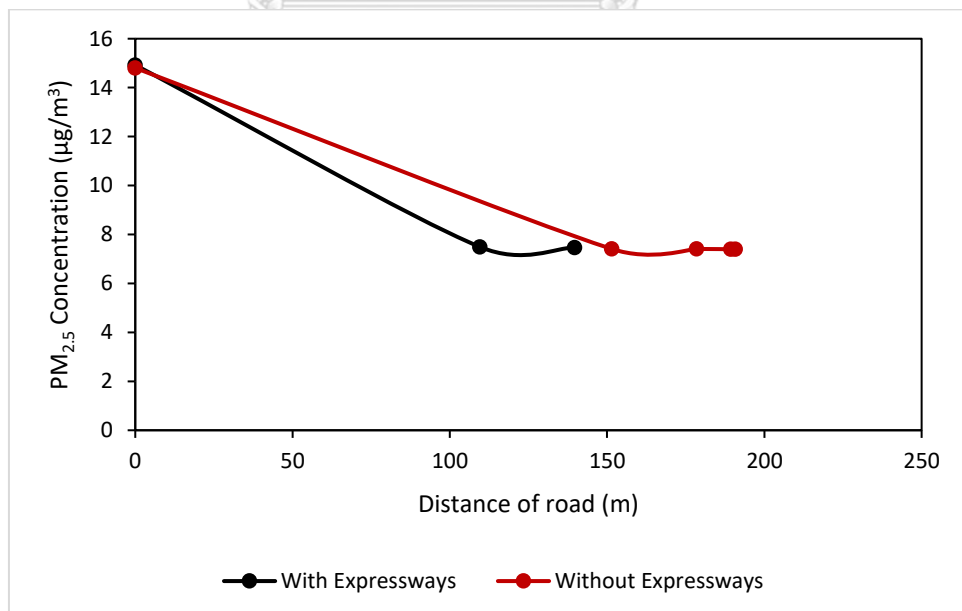


Figure 43: A Comparison of PM_{2.5} concentrations of both simulations at the locations where the PM_{2.5} concentrations were measured at different distances from the road.

Table 72: Comparative results of PM_{2.5} concentrations of both simulations at locations where PM_{2.5} concentrations were measured at different distances from the road.

Distance of road (m)	PM _{2.5} Concentration ($\mu\text{g}/\text{m}^3$)	
	With Expressways	Without Expressways
0	14.92	14.80
109.6	7.49	-
139.7	7.47	-
151.5	-	7.41
178.5	-	7.41
189.3	-	7.40
190.8	-	7.40

Note: The PM_{2.5} concentrations shown are multiplied by the correction factor equal to 0.00326.

From Figure 43, on the roadside, the concentration of PM_{2.5} decreases as the distance from the road increases, and from Figure 42, on both sides are tall buildings blocking the direction of the wind. PM_{2.5} is not blown away, causing the PM_{2.5} concentration to rarely change.

4.3 The influence of the city lockdown due to COVID-19 pandemic

The lockdown due to the COVID-19 pandemic directly affects the amount of traffic passing through the city (J. Du et al., 2021). The effects of the COVID-19 pandemic are being investigated. The simulation results are shown as follows.

Table 73: Comparative results of PM_{2.5} concentration during normal and lockdown periods.

Time	PM _{2.5} Concentration ($\mu\text{g}/\text{m}^3$)	
	Normal	Lockdown
7 AM - 9 AM	33.98	3.12
10 AM - 12 PM	28.46	7.67
13 PM -16 PM	25.47	19.11

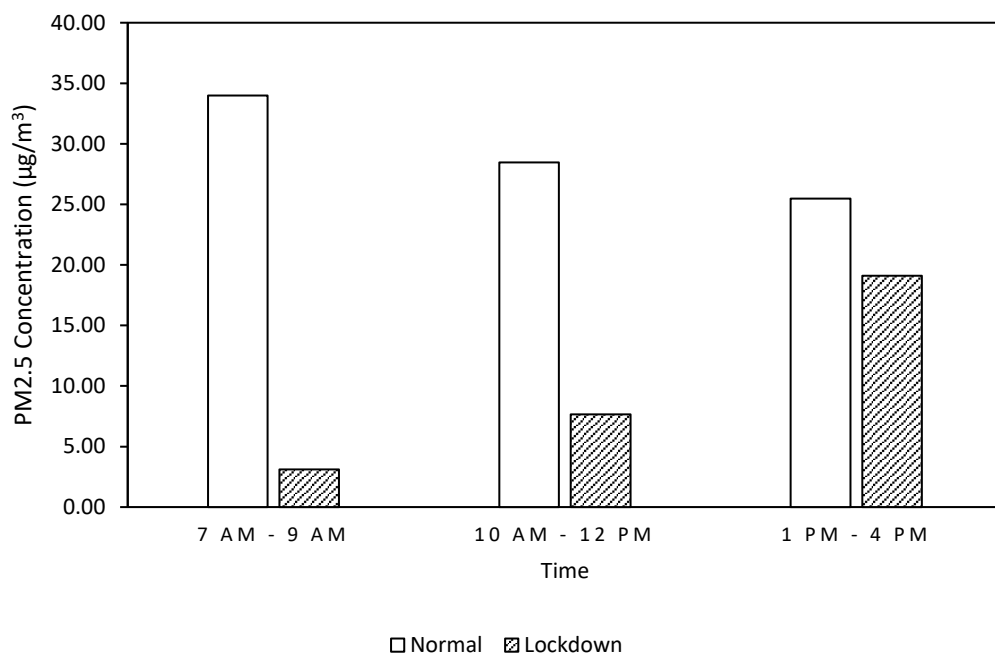


Figure 44 : PM_{2.5} concentration during normal and lockdown periods near the air quality monitoring station.

Figure 44 shows a comparison of PM_{2.5} concentrations during normal and lockdown periods near the air quality monitoring station. It was found that during the lockdown period, the concentration of PM_{2.5} decreased by approximately 63% compared to the normal period due to the emission rate during the lockdown period,

as shown in Table 76, being lower than the normal period by 20.54%. In addition, the high wind speed as shown in Table 74, particularly in the afternoon (1 PM – 4 PM) of the normal period might result in better ventilation and lower $PM_{2.5}$ concentration, despite the higher emission rate, in the afternoon. Furthermore, consider the trend of $PM_{2.5}$ concentrations during the lockdown period during which the temperature and wind speed are lower compared with the condition during the normal period. The increase of temperature and wind speed in the afternoon during the lockdown period might not sufficiently promote the atmospheric convection to reduce $PM_{2.5}$ accumulation (Li, 2015). Thus, $PM_{2.5}$ concentration during the lockdown period is increased with the emission rate.

Table 74: Wind speed and wind direction for three periods of normal and lockdown periods.

Time	Wind Speed (m/s)	
	Normal	Lockdown
7 AM – 9 AM	0.2	0.1
10 AM – 12 PM	0.43	0.2
1 PM – 4 PM	0.775	0.45

Table 75: Wind speed and wind direction for three periods of normal and lockdown periods.

Time	Temperature (K)	
	Normal	Lockdown
7 AM – 9 AM	300.52	299.75
10 AM – 12 PM	305.92	303.72
1 PM – 4 PM	306.43	305.70

Table 76: Emission rate, normal and lockdown periods.

Sources	Emission rate (kg/s)					
	Normal			Lockdown		
	7 AM – 9 AM	10 AM – 12 PM	1 PM – 4 PM	7 AM – 9 AM	10 AM – 12 PM	1 PM – 4 PM
Din Daeng rd.	5.53E-06	5.82E-06	8.74E-06	3.44E-06	4.75E-06	7.13E-06
Pracha Songkhro rd.	1.16E-06	1.72E-06	2.58E-06	7.29E-07	1.40E-06	2.11E-06
Mitmaitri rd.	1.09E-06	1.38E-06	2.08E-06	6.82E-07	1.13E-06	1.70E-06
Chalerm Mahanakorn Expr.	1.18E-06	1.18E-06	1.77E-06	9.71E-07	9.71E-07	1.46E-06
Si Rat Expr.	1.09E-05	1.09E-05	1.64E-05	8.98E-06	8.98E-06	1.35E-05
Total emission rate	1.99E-05	2.10E-05	3.15E-05	1.48E-05	1.72E-05	2.59E-05

Chapter 5

Conclusion

The study "Investigation of PM_{2.5} dispersion in Din Daeng district, Bangkok using Computational Fluid Dynamics modeling" aims to investigate PM_{2.5} dispersion. There are two cases in the simulation:

Case 1 Simulates the presence and absence of the COVID-19 pandemic.

In the absence of the COVID-19 pandemic, the data of January 27, 2020, will be used in the simulation and compared with the simulation results. During the COVID-19 pandemic, the data of January 25, 2021, will be used to compare how the results are different.

Case 2 Simulates the presence and absence of expressways.

The presence of expressways in the area results in more traffic flowing through the area. Therefore, in this study, the presence and absence of expressways will affect the concentration of PM_{2.5}.

The simulation results are divided as follows.

5.1 Validation Modal

The results concluded that the results obtained from the simulation tended to be consistent with the measured data. For example, PM_{2.5} concentrations at normal periods can be seen that the trend of PM_{2.5} concentrations obtained from the air quality monitoring station and simulation tends to decrease. As for the PM_{2.5} concentration in the lockdown period, it tends to increase the PM_{2.5} concentration obtained from the air quality monitoring station and the simulation. The acceptable error percentage is approximately 5-10%, depending on the application. However, the trend between simulation and experimental values should be the same (Kumar &

Veeman, 2020). In this study, both cases tended to be the same as the air quality monitoring stations, but most of the simulation values were greater than the measured data due to simplify the geometry to enable mesh generation.

5.2 Studies on the dispersion of PM_{2.5} when there are expressways.

The results of the simulation indicate that the PM_{2.5} concentrations obtained from the air quality monitoring station, the results from the simulation in the case of expressways, and the results from the simulation without expressways tend to decrease. By comparing the case with and without expressways, it was found that the presence of the expressway increased the concentration of PM_{2.5} by approximately 3.4 times compared to the case of no expressways. And the increase in the emission rate through the area will result in an increase in the concentration of PM_{2.5}. The peak time of the PM_{2.5} concentration is between 1 PM - 4 PM, which is the highest emission rate.

5.3 Studies on the dispersion of PM_{2.5} during normal and lockdown periods.

The simulation results concluded that during the lockdown period, the concentration of PM_{2.5} was reduced by approximately 63% compared to the normal period, due to the emission rate during the lockdown period being lower than the normal period by 20.54%. In other words, reducing traffic can reduce the concentration of PM_{2.5} in urban areas. The concentration of PM_{2.5} is also directly impacted by the meteorological conditions such as wind speed, and temperature.

5.4 Propose a guideline solution.

According to the simulation results of the reduction approach in the district that is similar to the Din Daeng district, it composed of residential buildings, government offices, educational institutions, and commercial areas. Din Daeng's overall area is composed of buildings that are not particularly tall. However, the building density is high, and the streets are relatively narrow. The PM_{2.5} reduction approach is to avoid construction that obstructs air flow, especially the construction of high-rise buildings adjacent to the expressway. Expressway surrounded by high-rise buildings will cause PM_{2.5} to accumulate within the area and make it difficult to diffuse out of the area. The area of high-rise buildings should be considered that it should be constructed in an open, well-ventilated area.

According to the simulation results, the concentration of $PM_{2.5}$ decreases as the distance from the road increases. Therefore, the distance between the main road and the building should be set for human health. From the simulation, it was also found that the amount of traffic affects the concentration of $PM_{2.5}$ in the urban areas. Therefore, it could be suggested that $PM_{2.5}$ reduction might be accomplished by developing a policy to control the amount of traffic during low wind speed. For example, when low wind speeds or high traffic volumes, the concentration of $PM_{2.5}$ is high, hence the idea is to limit the number of vehicles entering the city during those times. Passenger cars will represent the majority of vehicles in each time. Thus, there is a policy to encourage people to use electric cars more frequently, as well as the development of public transportation to provide people with additional incentives to utilize the transportation system. Improvements in oil quality, strict vehicle aged and combustion efficiency, may help reduce $PM_{2.5}$ concentrations.

5.5 Limitations

This study has limitations in terms of insufficient data. The limit of traffic data is only for one day. For meteorological data, only one air quality monitoring station in the study area, therefore, there are limitations to the meteorological data used as boundary conditions. This may not be very comprehensive. Therefore, more actual measurements or included in the study meteorological information from neighbouring districts that may have an impact on how $PM_{2.5}$ is dispersed in the future would make this study more accurate.

REFERENCES

- 6, R. E. O. (2009). *Principle of air sampling station installation*. <http://reo06.mnre.go.th>.
- (BORA), T. B. o. R. A. (2020). *Population and House Statistics - Population by age*.
http://stat.dopa.go.th/stat/statnew/upstat_age.php.
- Administration, S. a. E. D. B. M. (2019-2021). *Statistical Profile of Bangkok Metropolitan Administration*.
- ANSYS, I. (2003). *ANSYS FLUENT 12.0 Theory Guide*.
<https://www.afs.enea.it/project/neptunius/docs/fluent/html/th/node241.htm>.
- Daniel(Jian) Sun, & Zhang, Y. (2018). Influence of avenue trees on traffic pollutant dispersion in asymmetric street canyons: Numerical modeling with empirical analysis. *Transportation Research Part D: Transport and Environment*, 65, 784-795. <https://doi.org/10.1016/j.trd.2017.10.014>.
- Department, P. C. (2019-2021a). *Air quality in the area around Din Daeng Road, Din Daeng District, Bangkok in 2019-2021*.
<http://air4thai.pcd.go.th/webV2/region.php?region=1>.
- Department, P. C. (2019-2021b). *Meteorological Data*.
- Department, P. C. (2020). *Improving the standard for dust particles up to 2.5 microns in size in the general atmosphere*.
- Department, T. a. T. (2019-2021). *Traffic volume*.
- EMEP/EEA. (2006). *Air pollutant emission inventory guidelinebook*.
- Eric R. Pardyjak, a. M. J. B. (2001). *Evaluation of a fast response urban wind model-comparison to single building wind-tunnel data at the 3rd International Society of Environmental Hydraulics Conference, Tempe, Arizona*.
- H.H. Niu, B.Q. Wang, B.W. Liu, Y.H. Liu, J.F. Liu, & Wang, Z. B. (2018). Numerical simulations of the effect of building configurations and wind direction on fine particulate matters dispersion in a street canyon. *Environmental Fluid Mechanics*, 18, 829-847. <https://doi.org/10.1007/s10652-017-9563-7>.

- Hao Zhang, Yuxiang Wang, Shun Li, & Tang, H. (2015). Study on the Influence of the Street Side Buildings on the Pollutant Dispersion in the Street Canyon. *Procedia Engineering*, 121, 37-44. <https://doi.org/10.1016/j.proeng.2015.08.1016>.
- Hong, B., Lin, B., & Qin, H. (2017). Numerical investigation on the coupled effects of building-tree arrangements on fine particulate matter (PM_{2.5}) dispersion in housing blocks. *Sustainable Cities and Society*, 34, 358-370. <https://doi.org/10.1016/j.scs.2017.07.005>.
- J. Du, H.A. Rakha, F. Filali, & Eldardiry, H. (2021). COVID-19 pandemic impact on traffic system delay fuel, consumption and emissions. *International Journal of Transportation Science and Technology*, 10, 194-196. <https://doi.org/10.1016/j.ijtst.2020.11.003>.
- Jandaghian, Z. (2018). Flow and Pollutant Dispersion Model in a 2D Urban Street Canyons Using Computational Fluid Dynamics. *Computational Engineering and Physical Modeling* 1(1), 83-93. <https://doi.org/10.22115/CEPM.2018.122506.1014>.
- Krerkkaiwal, R. (2000). *Element composition of airborne fine particulate matter PM_{2.5} in Bangkok* Chulalongkorn University.
- Kumar, P. M., & Veeman, D. (2020). *How much variation between experimental and Computational Fluid Dynamics (CFD) Simulation results is acceptable ?* Retrieved from <https://www.researchgate.net/post/How-much-variation-between-experimental-and-Computational-Fluid-Dynamics-CFD-Simulation-results-is-acceptable/607580c524ef4d5fc2779408/citation/download>.
- Li, J., Chen, H., Li, Z. et al. (2015). Low-level temperature inversions and their effect on aerosol condensation nuclei concentrations under different large-scale synoptic circulations. *Advances in Atmospheric Sciences*, 32, 898–908. <https://doi.org/https://doi.org/10.1007/s00376-014-4150-z>.
- Luz T Padró-Martínez, Allison P Patton, Jeffrey B Trull, Wig Zamore, Doug Brugge, & Durant, J. L. (2012). Mobile monitoring of particle number concentration and other traffic-related air pollutants in a near-highway neighborhood over the course of a year. *Atmospheric Environment*, 46(61), 253-264. <https://doi.org/10.1016/j.atmosenv.2012.06.088>.

- McLean, D. (2012). *Understanding Aerodynamics: Arguing from the Real Physics*.
<https://doi.org/10.1002/9781118454190>.
- Narut Sahanavin, Kraichat Tantrakarnapa, & Prueksasit, T. (2016). AMBIENT PM 10 AND PM 2.5 CONCENTRATIONS AT DIFFERENT HIGH TRAFFIC-RELATED STREET CONFIGURATIONS IN BANGKOK, THAILAND. *Southeast Asian J Trop Med Public Health*, 47(3), 528-535.
- Pollution Control Department, C. R. I., and Department of Health. (2018). *Air Quality Assessments for Health and Environment Policies in Thailand*.
https://www.pcd.go.th/wp-content/uploads/2021/10/pcdnew-2021-10-28_04-12-33_133858.pdf.
- Salim Mohamed Salim, Riccardo Buccolieri, Andrew Chan, & Sabatino, S. D. (2011). Numerical simulation of atmospheric pollutant dispersion in an urban street canyon: Comparison between RANS and LES. *Journal of Wind Engineering and Industrial Aerodynamics* 99 103-113. <https://doi.org/10.1016/j.jweia.2010.12.002>.
- Sukko, O. (2020). *Where does Bangkok dust come from? If you want to manage the dust in Bangkok, where should you start from first?* Retrieved 11 from <https://theactive.net/data/pm-pollution-source/>.
- Sun, D., & Zhang, Y. (2018). Influence of avenue trees on traffic pollutant dispersion in asymmetric street canyons: Numerical modeling with empirical analysis. *Transportation Research Part D: Transport and Environment*, 65, 784-795.
<https://doi.org/10.1016/j.trd.2017.10.014>.
- SUPERSTRUCTURE RAILWAY OF BANGKOK. (2017).
<http://kmrailways.blogspot.com/2017/06/blog-post.html>.
- T.R., O. (1998). Street design and urban canopy layer climate. *Energy and Buildings*, 103-113.
- Talbot, L., Cheng, R. K., Schefer, R. W., & Willis, D. R. (2006). Thermophoresis of particles in a heated boundary layer. *Journal of Fluid Mechanics*, 101(4), 737-758.
<https://doi.org/10.1017/S0022112080001905>.
- Transport Statistics Sub-Division, P. D., Department of Land Transport. (2021). *Number of Vehicle Registered in Bangkok as of 31 December*.

- Ville Miettinen, U. E. P. A. (2019). *What is PM_{2.5} and Why You Should Care*.
<https://blissair.com/what-is-pm-2-5.htm>.
- Walaipan.Y. (2018). *Impact of traffic conditions on PM_{2.5} concentrations at two distinct traffic junctions*.
- X. Xie, Z. Huang, & Wang, J. S. (2005). Impact of building configuration on air quality in street canyon. *Atmospheric Environment*, 39, 4519-4530.
<https://doi.org/10.1016/j.atmosenv.2005.03.043>.
- Xiaoxia Wang, Xiaomei Yang, Xiaofei Wang, Jiahong Zhao, Sangen Hu, & Lu, J. (2020). Effect of reversible lanes on the concentration field of road-traffic-generated fine particulate matter (PM_{2.5}). *Sustainable Cities and Society*, 62, 102389.
<https://doi.org/10.1016/j.scs.2020.102389>.
- Y. Nakamura, & Oke, T. (1988). Wind, temperature and stability conditions in an east-west oriented urban canyon. *Atmospheric Environment (1967)*, 22(12), 2691-2700. [https://doi.org/10.1016/0004-6981\(88\)90437-4](https://doi.org/10.1016/0004-6981(88)90437-4).



จุฬาลงกรณ์มหาวิทยาลัย
CHULALONGKORN UNIVERSITY

VITA

NAME Amintra Tancharoen
DATE OF BIRTH 12 October 1997
PLACE OF BIRTH Samut Prakarn
INSTITUTIONS ATTENDED B.Eng
HOME ADDRESS 62/270 Moo.6 Soi Rewat 12 Bang Mueang Mai, Muang
Samut Prakarn, Samut Prakan, 10270



จุฬาลงกรณ์มหาวิทยาลัย
CHULALONGKORN UNIVERSITY